Modelling of soil water content and soil salinity with *HYDRUS-1D*

João Francisco dos Santos Antunes

Dissertação para a obtenção do Grau de Mestre em

Engenharia Agronómica

Orientadores: Dr. Nuno Renato da Silva Cortez

Dra. Ana Marta Marques Duarte da Paz

Júri: Presidente: Dr. Carlos Manuel Antunes Lopes, Professor Associado com Agregação do Instituto Superior de Agronomia da Universidade de Lisboa

Vogais: Dra. Paula Cristina Santana Paredes, Professor Auxiliar do Instituto Superior de Agronomia da Universidade de Lisboa

Dra. Ana Marta Marques Duarte da Paz, Técnica Superior do Instituto Nacional de Investigação Agrária e Veterinária

2023

Acknowledgements

This thesis stands as a testament to the extraordinary mentorship and unwavering support of my supervisors, Dr. Nuno Cortez and Dra. Ana Marta Paz. I would like to express my most sincere gratitude to them, but not only.

To INIAV, which became my second home during these months and the project *SoilSalAdapt* (DOI 10.54499/EJPSoils/0003/2021), financed by Fundação para a Ciência e Tecnologia (FCT), which provided me room for new experiences and discussion of ideas.

To Dr. Maria Conceição Gonçalves, Dr. Nádia Castanheira and Dr. Tiago Ramos for discussing outcomes, the encouragement, and the review of the work.

To Santander Totta who awarded me the Santander Universities/Instituto Superior de Agronomia prize, which made me feel recognized for my academic merit.

To my family for their support and for being there for me, even when I was stressed about this huge chapter in my life.

Last but not least, I would like to thank Mariana, for all the patience she has with me and my crisis of overthinking, for reviewing the thesis and for all the moments of distraction and happiness provided during these months of this work.

Abstract

Salt-affected soils may result in highly negative impacts on the soils' functions, limiting the soils' productivity and ultimately leading to desertification. The area of salt-affected soils is increasing globally as a result of inadequate irrigation practices and of climate change.

This work was carried out within the *SoilSalAdapt* project, which studies the hypothesis that adaptation of soil microbiome to soil salinity may result in increased crop tolerance. The aim of this work was to model the soils' water content and soil salinity in the three different soils used in the experiment carried out by the project team at the Lincoln University, UK. In experiment, spinach was grown in vases, without fertilization, inside a polytunnel, during two growth cycles. Spinach was irrigated with non-saline water and, at the end of the second cycle, with highly-saline water.

In this work, *SIMDualKc* was used to calculate crop evapotranspiration under standard conditions using the dual crop coefficient method. *HYDRUS-1D* was used to model the soil water content and electrical conductivity of soil water, integrating water and salinity stresses to obtain the actual crop evapotranspiration. The models resulted in a root mean square error between 0.024 and 0.063 cm^3cm^{-3} for soil water content and between 1.74 and 3.31 dSm^{-1} for soil salinity. The errors were lower when considering only the first growth cycle. At the end of the second cycle, when saline water was applied, the models underestimated the water content and overestimated the salinity. These larger errors reflect the fact that observed data, which was measured with a TDR, overestimated the soil water content when soil salinity was high.

The models obtained in this thesis will allow the simulation of soil salinity under short- and long-term conditions, considering different irrigation managements and future climate conditions, and the estimation of potential productivity losses.

Key-words: soil, salinity, modelling, *SIMDualKc, HYDRUS-1D*

Resumo

A salinidade pode afetar os solos resultando em impactos negativos nas funções do solo, limitando a sua produtividade e podendo levar à desertificação. A área afetada pela salinidade está a crescer mundialmente, resultado de uma gestão inadequada da rega e das alterações climáticas.

Este trabalho foi feito no âmbito do projeto *SoilSalAdapt*, que estuda a hipótese de pré-adaptar o microbioma à salinidade do solo através da gestão da salinidade da rega, conferindo tolerância às culturas. O objetivo deste trabalho é modelar o teor de água do solo e a salinidade em três tipos de solo usados na experiência efetuada pela equipa da Universidade de Lincoln. Na experiência, espinafres cresceram em vasos dentro de uma estufa, sem fertilização, durante dois ciclos de crescimento. Foram regados com água não salina e no final do segundo ciclo com água extremamente salina.

Foi usado o *SIMDualKc* para calcular a evapotranspiração cultural em condições padrão usando a metodologia dos coeficientes duais. O *HYDRUS-1D* foi usado para modelar o teor de água do solo e a condutividade elétrica da água do solo, integrando o stress salino e hídrico, para obter a evapotranspiração cultural real. A raiz do erro quadrático médio foi de 0,024 a 0,063 cm^3cm^{-3} para o teor de água e entre 1,74 até 3,31 dSm^{-1} para a salinidade. Os erros foram mais baixos no primeiro ciclo quando comparados com o segundo. No final do segundo ciclo, quando a rega salina é aplicada, os modelos subestimam o teor de água do solo e sobrestimam a salinidade. Estes erros superiores devem-se aos dados medidos com o TDR, que sobrestimam o teor de água no solo quando a salinidade é elevada.

Os modelos obtidos permitem simular a salinidade a curto e longo prazo, considerando diferentes gestões de regas e alterações climáticas, e estimar potenciais perdas de produtividade.

Palavras-chave: solo, salinidade, modelação, *SIMDualKc*, *HYDRUS-1D*

Resumo alargado

O presente trabalho tem como objetivo modelar o teor de água e salinidade do solo em três tipos de solo durante o crescimento de espinafre em vasos, usando a ferramenta *HYDRUS-1D*. O trabalho foi realizado no âmbito do projeto *SoilSalAdapt* - Preadaptação do microbioma do solo para uma maior tolerância à salinidade do solo, coordenado pela Universidade de Lincoln no Reino Unido em parceria com a Universidade de Oslo na Noruega e o Instituto Nacional de Investigação Agrária e Veterinária. O projeto coloca a hipótese de que poderá ser possível pré-adaptar as comunidades microbianas à salinidade do solo através da gestão da salinidade da rega. Esta hipótese será estudada em ensaios com rega de salinidade gradualmente mais elevada, analisando os impactos ao nível do microbioma do solo e da produtividade das culturas.

Os solos podem ser afetados por diferentes desequilíbrios iónicos. A salinidade representa um desses casos, traduzido por uma elevada concentração de sais solúveis na solução do solo. A salinidade do solo pode ter causas naturais (processos primários), como por exemplo a acumulação de sais ao longo do perfil de solo decorrente da subida de águas subterrâneas naturalmente salinas ou causas antropogénicas (processos secundários), como por exemplo a gestão incorreta da rega e drenagem.

A salinidade pode resultar na degradação do solo, afetando as plantas e o ecossistema e podendo, em último caso, conduzir à desertificação. A salinidade do solo dificulta a absorção de água e de nutrientes pelas plantas, podendo colocá-las em stress hídrico e défice nutricional, ou ainda provocar toxicidade resultante da elevada concentração de alguns iões, tais como o sódio ou o cloro. A sensibilidade das culturas à salinidade do solo depende de vários fatores, tais como a espécie e variedade da planta, bem como o seu sistema radicular, mas também poderá depender das condições do solo, inclusive o microbioma. O parâmetro mais utilizado para expressar a salinidade do solo é a condutividade elétrica.

As alterações climáticas agravam alguns dos fatores que estão na origem da salinidade do solo. O aumento da temperatura média e a diminuição da precipitação em algumas regiões, como é o caso da região mediterrânica, resulta numa redução da capacidade de lavagem natural dos sais para camadas do solo abaixo da zona radicular. Por outro lado, a subida do nível de água do mar aumenta o risco de intrusão salina nos solos de zonas costeiras, afetando áreas com vários climas. A área de solos afetados por sais tem vindo a aumentar a nível global. Na região mediterrânica, deve-se sobretudo à gestão inadequada da rega. Processos primários de salinização em Portugal ocorrem em zonas costeiras, como por exemplo na Lezíria Grande de Vila Franca de Xira, enquanto que os processos secundários podem ocorrer em áreas regadas, sobretudo no sul do país. Fora da

zona mediterrânica, tal como no Reino Unido e na Noruega, a salinidade da água de rega tem aumentado, devido a processos primários, nomeadamente a intrusão salina.

O presente trabalho é baseado no ensaio experimental realizado pela equipa do projeto na Universidade de Lincoln, estando a sua implementação e monitorização fora do trabalho da dissertação. O ensaio foi realizado numa estufa, em três tipos distintos de solo: dois solos franco-arenosos e um solo franco. Foram feitas duas sementeiras sucessivas de espinafre, planta que possui uma tolerância moderada à salinidade. Os dois ciclos culturais foram regados com água com uma condutividade elétrica de 0 dSm^{-1}. O primeiro ciclo teve uma duração de 34 dias e o segundo ciclo de 36 dias. Dezasseis dias antes do final do segundo ciclo, a rega passou a ser feita com água com uma condutividade elétrica elevada, igual a 9 dSm^{-1}. Foram recolhidos dados do ensaio necessários para a modelação tais como as dotações de rega e precipitação, a temperatura, a humidade relativa do ar, o teor de água e a condutividade elétrica do solo, monitorizados duas vezes por semana, utilizando um equipamento TDR.

Usou-se o software *SIMDualKc* para calcular a evapotranspiração do espinafre em condições padrão, usando o método dos coeficientes culturais duais. Este método permite uma melhor estimativa, em culturas regadas, da evaporação e transpiração cultural. Para o cálculo da evapotranspiração de referência, usou-se o método de Hagreaves-Samani, que confere boas estimativas em condições controladas como em estufa. Para a estimativa da fração coberta do solo, utilizou-se o programa *Canopeo*, que confere boas estimativas para a fração coberta com base em registos fotográficos. Os outros dados de entrada foram obtidos por medição direta ou por consulta bibliográfica.

Com a evaporação e transpiração em condições padrão, estimadas pelo *SIMDualKc*, procedeu-se à modelação do teor de água e da condutividade elétrica da água do solo no programa *HYDRUS-1D*, sendo modelados os stresses hídrico e salino, que reduzem ou inibem a absorção de água pelas raízes. Ambos os stresses foram modelados com parâmetros específicos para a cultura do espinafre. Assumiram-se como condições fronteira a drenagem livre para a fronteira inferior e as condições atmosféricas como fronteira superior. Relativamente ao modelo hidráulico optou-se pelo modelo de van Genucthen-Mualen, sendo os parâmetros necessários ajustados por modelação inversa. Quanto à modelação da condutividade elétrica da água do solo, a condição fronteira inferior foi de um gradiente de concentração de zero e a condição fronteira superior foi considerada um fluxo, que neste caso, corresponde à condutividade da água de rega.

No decorrer do ensaio pelo parceiro do projeto, verificou-se que os valores do teor de água medidos pelo TDR eram muito sobrestimados quando a condutividade elétrica do solo

era mais elevada, nomeadamente no período de rega com 9 dSm^{-1}. De forma a poder usar os dados do ensaio, foi feita uma correção dos valores do teor de água. Para essa correção, determinou-se o teor de água em algumas amostras de solo dos vasos pelo método gravimétrico e realizaram-se regressões entre o teor de água medido pelo TDR e pelo método gravimétrico. Regressões logarítmicas para cada um dos tipos de solo, resultaram em coeficientes de determinação elevados (R^2> 0.76), indicado uma boa correlação. A correção dos dados do teor de água no solo com as regressões logarítmicas permitiu reduzir o erro dos dados observados. Os resultados da modelação do teor de água e salinidade do solo no *HYDRUS-1D* mostram que os modelos estão bem ajustados aos dados observados para os três tipos de solo. No final do segundo ciclo de crescimento do espinafre, quando ocorre a rega de salinidade elevada e a salinidade do solo aumenta, os modelos subestimam o teor de água para todos os tipos de solo e sobrestimam a condutividade elétrica da água do solo. Estas diferenças devem-se ao facto de, apesar da correção dos valores do teor de água medidos pelo TDR, continua a haver uma sobrestimativa do teor de água observado para condutividades elétricas mais elevadas. A raiz do erro quadrático médio foi de 0,024 a 0,063 cm^3cm^{-3} para o teor de água e entre 1,74 até 3,31 dSm^{-1} para a salinidade. Para o primeiro ciclo do espinafre foi entre 0.02 e 0.03 cm^3cm^{-3} para os três tipos de solo e no segundo ciclo entre 0.03 e 0.08 cm^3cm^{-3}. No caso da condutividade elétrica, o erro quadrático médio foi entre de 0.91 e 1.65 dSm^{-1} no primeiro ciclo e entre 2.21 e 4.24 dSm^{-1} no segundo ciclo.

A água extraída pelas raízes, resultado dos modelos obtidos no *HYDRUS-1D*, mostrou que o efeito do stress hídrico e salino resulta numa diferença entre a água potencialmente extraída pelas raízes, ou seja, em condições padrão, e a água realmente extraída pelas raízes, ou seja, em resultado da aplicação de ambos os stresses. Observando os valores de água realmente extraída pelas raízes e da água drenada (também obtida através dos modelos do *HYDRUS-1D*), verifica-se que as saídas de água no sistema são quase nulas no final do segundo ciclo de crescimento de crescimento do espinafre. Nesta fase do ciclo, apesar das saídas de água serem quase nulas e de existir rega, não é possível modelar teores de água tão elevados como os observados. Este resultado indica que o teor de água observado nesta fase do ciclo continua a ter um erro de sobrestimativa, apesar da correção.

Nos próximos passos do projeto, devem ser recolhidos mais dados relativos à cultura (como a altura das plantas e profundidade das raízes), ao solo (como é o caso de alguns pontos da curva de retenção de água), assim como mais dados meteorológicos no interior da estufa, de modo a obter modelos mais precisos. A medição do teor de água deverá ser feita utilizando um método que permita medições mais precisas, mesmo em condições de salinidade elevada. Deve-se ainda validar estes modelos utilizando dados de outras experiências.

Este trabalho permitiu desenvolver modelos com baixos erros, que permitirão simular a curto e longo prazo os efeitos da qualidade da água de rega e das condições climáticas futuras na salinidade do solo, estimando eventuais perdas de produtividade.

Table of Contents

List of figures

List of tables

List of abbreviations

ϕ	$[ML^{-3}T^{-1}]$	Sink-source term in transport solutes equation
μ	[-]	Root-water uptake water stress response function
α	$[L^{-1}]$	van Genuchten parameter
β	$[L^{-1}]$	Normalized root density
θ	$[L^3L^{-3}]$	Volumetric soil water content
θ_r	$[L^3L^{-3}]$	Residual volumetric water content
θ_s	$[L^3L^{-3}]$	Saturation volumetric water content
ρ	$[ML^{-3}]$	Bulk density
τ	[-]	Transmissibility factor

A_t	$[L^2]$	Area of the soil surface associated to transpiration
c	$[ML^{-3}]$	Solute concentration
D	$[L^2T^{-1}]$	Dispersion coefficient
$D_{e,\ i-1}$	$[LT^{-1}]$	Cumulative evaporative depletion of the previous day
E	$[LT^{-1}]$	Evaporation
EC	$[M^{-1}L^{-2}T^3A^2\ ]$ (dS/m)	Eletrical conductivity
EC_b	$[M^{-1}L^{-2}T^3A^2]$ (dS/m)	Bulk electical conductivity
Ec_e	$[M^{-1}L^{-2}T^3A^2]$ (dS/m)	Eletrical conductivity in the saturated soil paste
Ec_{sw}	$[M^{-1}L^{-2}T^3A^2\ ]$ (dS/m)	Electrical conductivity of the soil solution
ET_c	$[LT^{-1}]$	Crop evapotranspiration
ET_o	$[LT^{-1}]$	Reference evapotranspiration
f_c	[%]	Fractional vegetation cover
f_{ew}	[%]	Fraction of the soil that is both exposed and wetted
f_w	[%]	Fraction of soil surface wetted
h	[L]	Pressure head
h_e	[L]	Plant height
$h\ \phi$	[L]	Osmotic pressure
$h1$	[L]	Feddes parameter
$h2$	[L]	Feddes parameter
$h3h$	[L]	Feddes parameter
$h3l$	[L]	Feddes parameter
$h4$	[L]tortu	Feddes parameter
I	[-]	Tortuosity parameter
$K(h)$	$[LT^{-1}]$	Unsaturated hydraulic conductivity function
K_c	[-]	Crop coefficient
K_{cb}	[-]	Basal crop coefficient
$K_{cb(tab)}$	[-]	Reference basal crop coefficient
Kc_{max}	[-]	Maximum value of K_c following rain or irrigation
K_e	[-]	Soil evaporation coefficient
K_r	[-]	Evaporation reduction coefficient
n	[-]	van Genuchten parameter
q	$[LT^{-1}]$	Volumetric fluid flux density
r	$[L^3]$	Unit of soil
R_a	$[MT^{-3}]$ (MJ m^{-2} day^{-1})	Extra-terrestrial radiation
REW	[L]	Readily evaporable water

RH_{min}	[%]	Minimum relative humidity
$RMSE$	[-]	Root mean square error
S	[LT^{-1}]	Actual root water uptake
s	[-]	Adsorbed concentraion
S_p	[LT^{-1}]	Potential root water uptake
T	[°C]	Daily mean temperature
t	[T]	Time
TEW	[L]	Total evaporable water
T_{max}	[°C]	Maximum temperature of day
T_{min}	[°C]	Minimum temperature of day
T_p	[LT^{-1}]	Potential transpiration rate
T_r	[LT^{-1}]	Transpiration
u_2	[LT^{-1}]	Wind speed at 2 meters height
z	[L]	Vertical coordinate positive upward

1. Introduction

The aim of this thesis was to model the soil water content and soil salinity in three soil types during spinach growth cycles in large scale pots, using *HYDRUS-1D*.

The work was made in the scope of the project *SoilSalAdapt* - Preadapting soil biology for increased tolerance to elevated salinities due to climate change, coordinated by Lincoln University and with National Institute for Agricultural and Veterinary Research (INIAV) and Norwegian Faculty of Life Sciences as partners. The project proposes to study the hypothesis that soils' microbiome can adapt to increased soil salinity, through irrigation management, resulting in higher crop tolerance and minimizing potential productivity losses. The hypothesis is tested by carrying out experiments with different soils, crops, and irrigation treatments in Lincoln, UK.

The models developed in this thesis were based on the data of the experiments implemented in Lincoln, which implementation and data collection was outside the scope of the thesis. The models will allow the simulation of soil salinity under short- and long-term conditions, considering different irrigation managements and future climate conditions and to estimate potential productivity losses.

In this thesis, the software *SIMDualKc* was used to calculate the crop evapotranspiration under standard conditions using the dual coefficient method, which was used as input for modelling the soil water content and soil salinity during the spinach growth cycles using *HYDRUS-1D*.

The thesis is divided in five chapters: introduction presents the motivation of the work, literature review presents the theoretical background; materials and methods presents information about the experimental setup, the soils, and the input data used in the modelling tools; the last two sections present the results and discussion of the work and the conclusions.

2. Literature review

2.1 Salt-affected soils

Soils may be salt-affected due to salinity, sodicity, alkalinity or a combination of these situations. Salinity refers to the accumulation of water-soluble salts in the soil water, sodicity is the excess of sodium in the soils' exchange complex, and alkalinity occurs when the soils' pH increases above 7. Salt-affected soils may result in highly negative impacts on the soils' functions, limiting the soils' productivity and ultimately leading to desertification (Weil & Brady, 2017).

Salt-affected soils may arise as a result of primary or/and secondary processes. Primary processes are those with natural origin, such as the natural accumulation of salts at the soil surface without sufficient leaching by rainfall and the upward capillary flow from saline groundwater under circumstances of high evapotranspiration in arid and semi-arid regions. It may also be caused by the direct action of tides in coastal regions, deposition of marine salts transported by the wind or the intrusion of sea water in low areas. Secondary processes have anthropogenic origin, which are mainly due to inadequate management of irrigation and drainage and the intensive use of fertilizers (Gonçalves *et al.*, 2015).

This thesis focuses in irrigation-induced salinity. In arid and semi-arid conditions, the water is lost from the soil by evaporation / evapotranspiration but the salts remain in the soil and the occurred rainfall may not be sufficient to naturally leach the salts away from the rootzone to deeper soil layers. This problem is exacerbated when the used water has a high concentration of salts (Weil & Brady, 2017).

2.2 Effects of salt-affected soils

Excessive salt accumulation causes soil degradation, affecting the plants and the chemical and physical characteristics of the soil. Soil salinity affects plants due to the decrease of the soil osmotic potential of the soil water with the increase of salt concentration. As the osmotic potential lowers, it becomes more difficult for the roots to remove water from the soil. In addition, the high concentration of some ions, such as Na^+ and Cl^-, can cause toxicity to the plants and it may limit the absorption of necessary ions, due to competitive reactions such as the limitation of K^+ absorption in the excess of Na^+ (Weil & Brady, 2017).

When the soil develops sodicity, the particle aggregation can be compromised due to slaking, swelling, and dispersion of clay particles which may result in the destruction of the soil structure and reduction of the soils' permeability. Soil structure degradation increases the risk of soil erosion due to lower infiltration and higher surface runoff. The destruction of the soil structure and development of impermeable layers limits root and plant growth and may, in more severe cases, lead to desertification (Paz *et al.*, 2023).

In alkaline soils (pH>7), the bioavailability of macro and micronutrients may become limited, which can lead to deficiency or toxicity problems in plants. These processes may result in a more or less severe drop in crop productivity and consequent increase in production costs (Weil & Brady, 2017)

2.3 Salinization in world, Europe, and Portugal

Salt-affected soils exist in over 100 countries and there is no continent completely free of soil salinity. The most recent estimate of the affected area is the FAO Global Map of Salt-

affected Soils which estimates 4,24 x 10^{6} km^2 of topsoil (0-30 cm) and 8,33 x 10^{6} km^2 of subsoil (30-100 cm), distributed around the globe, but with two-thirds of the area located in arid and semi-arid (FAO, 2021a). The area of salt-affected soils is currently increasing, especially in irrigated soils (Machado & Serralheiro, 2017).

In Europe, especially in the Mediterranean region, soil salinity is increasing due to an increase of irrigation with low quality water (rich in salts). In the Mediterranean area, 25% of irrigated cropland is affected by moderate to high salinization (Joint Research Centre *et al.*, 2015). In Portugal, it is estimated that salt-affected soils are about 1,5 x 10^{9} km^2, mainly in coastal areas. Of these, 1,0 x 10^{9} km^2 are affected by primary salinization and the remaining area by the use of low-quality water and incorrect irrigation and drainage management. Secondary salinization occurs mainly in Alentejo region, due to the climatic conditions (dry sub-humid and semi-arid) and, in many cases, soils with low permeability, which limits leaching (Gonçalves *et al.*, 2015).

The risk of development salt-affected soils is also increasing outside the Mediterranean region. For example, in the west coast of England, the salinity of water available for irrigation of agricultural soil, has been increasing due to sea water intrusion. In the southeast coast of Norway, it has been registered a steep increase in the salinity of groundwater in high-productivity agricultural areas, which may lead to soil salinity in periods when a rise of the groundwater may occur (Gould *et al.*, 2021).

In the case of the United Kingdom, a study carried out in Lincoln by Gould *et al.* (2020), predicts that a coastal flooding event may result in a cost of 566.89 € km^{-2}. If a coastal flooding event occurs every 200 years, assuming no coastal defences, it could result financial losses of 115 to 555 million euros and production losses of 1.3 to 2.5 million tonnes. These costs relate to the total loss of the crop at the time of the flood and the decrease in productivity in the following years.

2.4 Climate change and salt-affected soils

Salt-affected soils are expected to increase in the near future considering the projected climate change scenarios. The projections for the Mediterranean region, indicate a decrease in precipitation, increase in mean temperature, and increase in sea water level. The climate change projections depend on the adopted scenarios. The IPCC 5th Assessment Report uses different scenarios to model the impacts of greenhouse gases concentration in the atmosphere, corresponding to representative concentration pathways (RCP) up to 2100. RCP 2.6 describes a scenario with very restricted emissions where emissions start to decline by 2020 and reach zero by 2100. Scenario 4.5 implies a decrease in emissions by 2040. Scenario

8.5 is the worst-case scenario, in which emissions continue to rise beyond the end of the century (IPCC, 2014).

Figure 1 shows the projection of the change in average annual temperature for Europe for IPCC scenarios RCP 4.5 and 8.5, according to EEA, (2021). Depending on the scenario, there is a projected increase between 2 and 4º C in Portugal. Figure 2 shows the projected changes in annual precipitation in Europe for RCP 8.5. Figure 2 shows that Portugal and the Mediterranean are among the regions in Europe with largest decrease in annual precipitation, and that it is projected a decrease of up to 30% in Portugal. The combined effect of increased temperature and decreased rainfall, will lead to larger evapotranspiration and less ability to naturally leach the salts from the rootzone, increasing the risk of developing salt-affected soils (Daliakopoulos *et al.*, 2016).

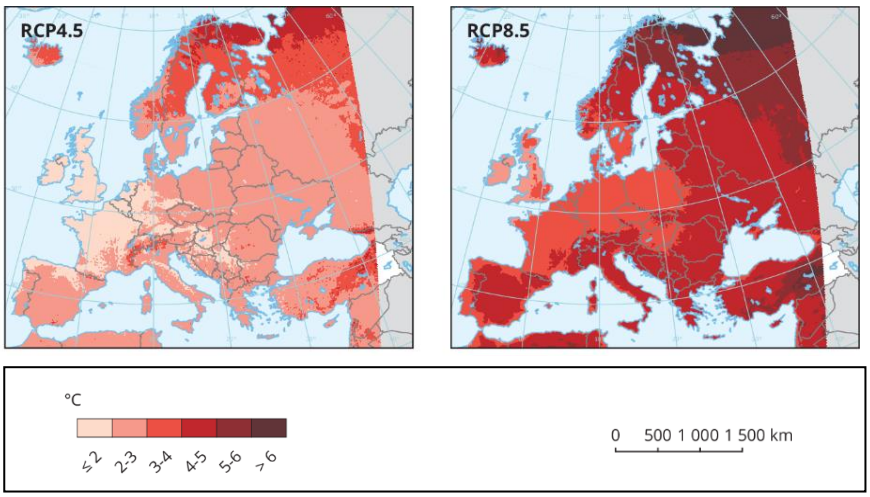

Figure 1: Projected change in average annual temperature in Europe for RCP 4.5 and 8.5. Source: (EEA, 2021)

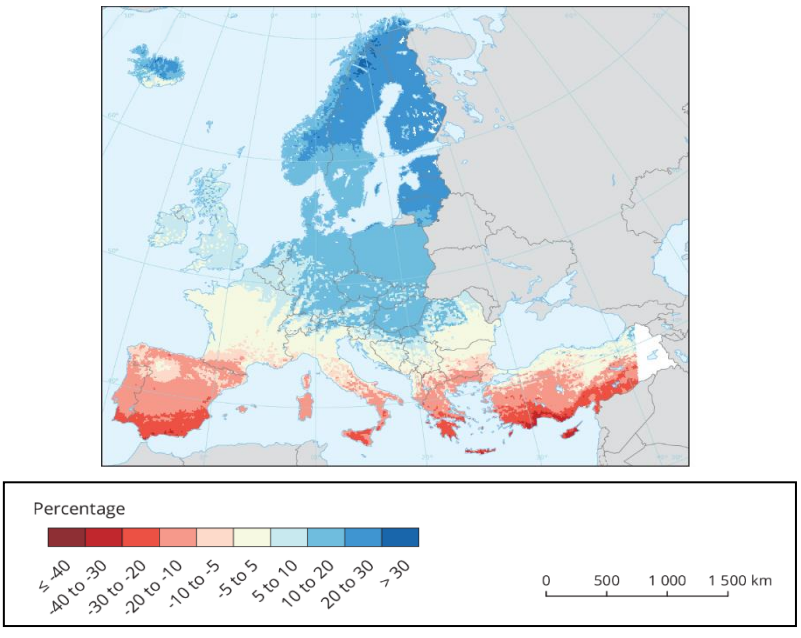

Figure 2: Projected changes in annual precipitation in Europe for the RCP 8.5. Source: (EEA, 2021)

Figure 3 shows the projected change in relative sea level in Europe for RCP 2.6 and 8.5. The figures show that in Portugal, it is projected that the sea level can rise between 0.2 and 0.6 meters until 2100, depending of the scenario (RCP 2.6 or RCP 8.5). The rise in sea water level leads to saline intrusion in coastal areas, contaminating the groundwater. The rise of the groundwater level and the capillary rise to the root zone may result in the development of salt-affected soils. Saline intrusion can also affect the salinity of the water used for irrigation, which is an increased risk for salt-affected soils, as described in section 2.1 (Daliakopoulos *et al.*, 2016).

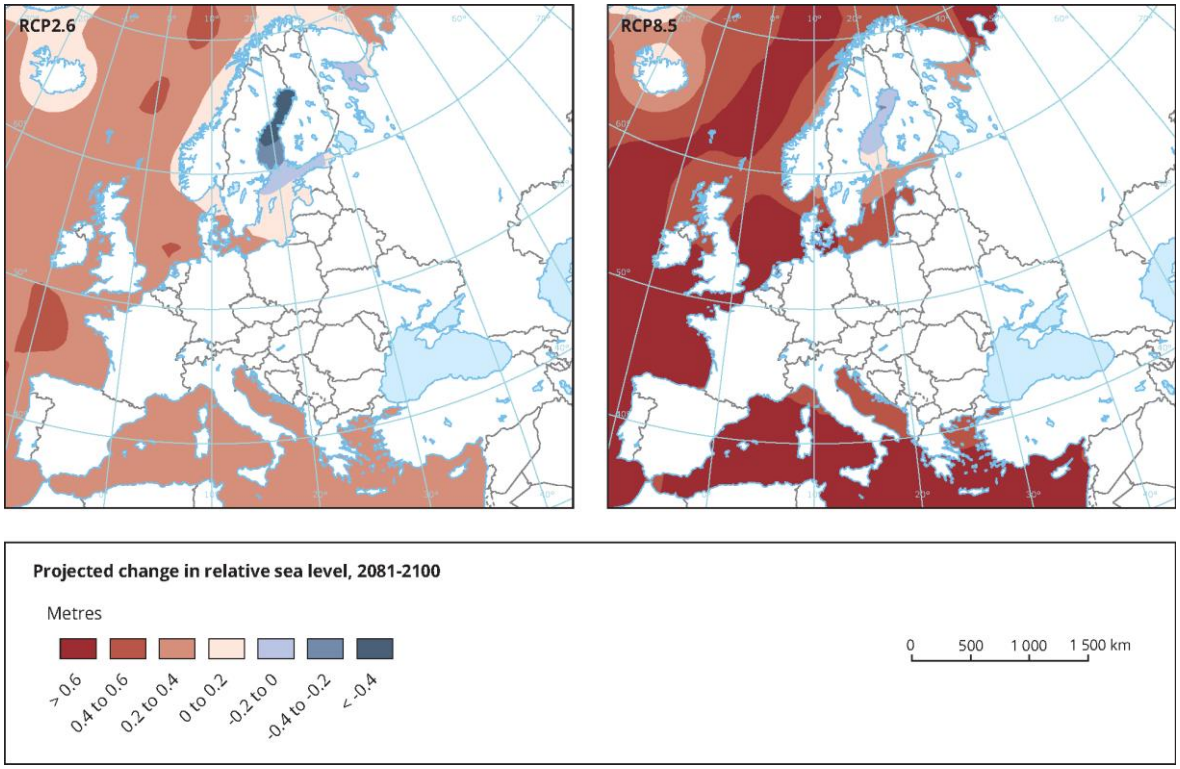

Figure 3:Projected change in relative sea level in Europe for RCP 2.6 and 8.5. Source: (EEA, 2021)

The projected climate change effects shown in figures 1 to 3, result in changes on land value, as shown in figure 4 (EEA, 2021). Figure 4 shows that in Portugal it is estimated a land value decreases between 40-60% in most of the area. This decrease considers the increase of salt-affected soils.

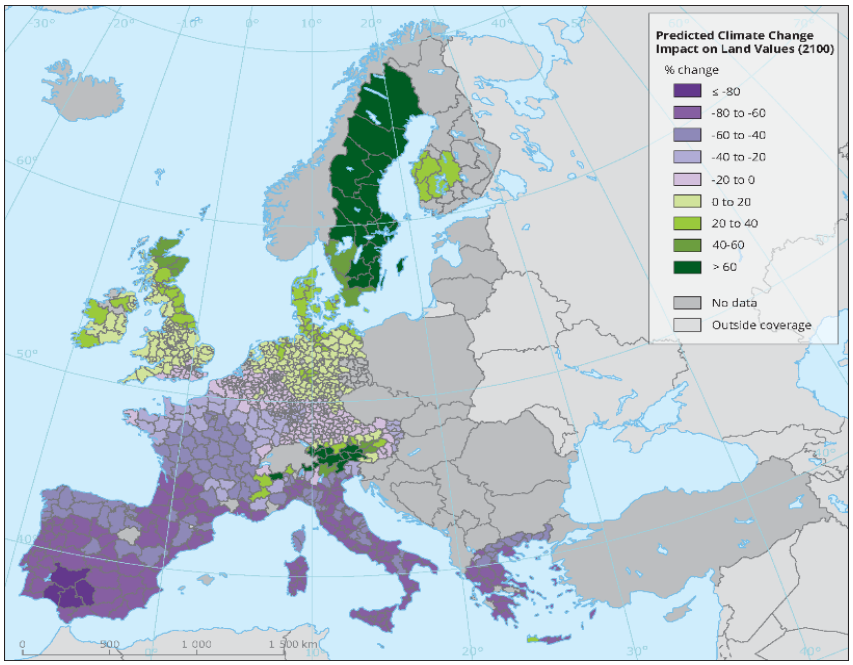

Figure 4: Predicted impact on land values under climate change scenarios. Source: (EEA, 2021)

These scenarios show that salt-affected soils will be a main cause of soil degradation in the Mediterranean region, and it is urgent to develop new strategies to overcome these new challenges.

2.5 Indicators of soil salinity

Electrical conductivity (*EC*) [dSm^{-1}] is preferentially used to express soil salinity due to its measurement simplicity. It is possible to measure the *EC* in aqueous extracts obtained from soil-water mixtures, such as 1:1, 1:2, and 1:5, or in a saturated soil paste. The *EC* of the soil solution (EC_{sw}) is the actual salinity encountered by crop roots; however, the plant's ability to extract soil water varies with specific soil properties and its value is affected by the actual soil water content. One advantage of determining *EC* in extracts of soil-water mixtures and in the saturated soil paste (EC_e) is the possibility of allowing comparison among samples, independent of the water content under field conditions. The EC_e is commonly used as a reference for evaluating soil salinity and the crops' sensitivity and response because it is closely related to EC_{sw} (Paz *et al.*, 2023).

The saturated soil paste extract is obtained by adding distilled water to a soil sample until the saturation point is reached. The saturation point is reached when three criteria are met: 1) the soil glistens as it reflects light, 2) flows slightly when the container is tipped, 3) slides freely and cleanly off the spatula. The method for obtaining the saturated soil paste has been initially published by Richards (1954) and includes a standing time of "one hour or more"

before rechecking the three criteria for saturation. After the standing time, more water can be added if the paste stiffens or loses glisten or more soil can be added if there is free water at the soil surface. The method for preparation of the saturated soil paste has been recently revised by FAO (2021b), which added an additional standing time of 24 hours and a further checking of the saturation criteria, but without providing support data regarding the relevance of this additional standing time. Antunes *et al.* (2023) studied the influence of the standing times in EC_e and EC_{sw} of three soil types and found no statistical difference in results when including the 24 h standing time.

The EC_e value of 4 dSm^{-1} is widely used by a threshold to classifying saline soils, according to Richards (1931), however the value of 2 dSm^{-1} is used to classified soils in Global Map of salt-affected soils FAO (2021b).

2.6 Crops' tolerance to soil salinity

Plants are able to extract water from the soil by maintaining a lower osmotic potential in root cells than in the soil solution. Higher concentrations of salts in the soil will lower the osmotic potential which causes the plant to expend more energy to absorb water. The plant has to accumulate solutes inside the cells in order to counterbalance the low osmotic potential of the soil solution. Additionally, more energy will also be needed to uptake nutrients from the soil, resulting in slower assimilation and, ultimately, in nutrient deficiency. Consequently, this loss of energy will be reflected in the growth, development, and productivity of the plant (Weil & Brady, 2017).

The sensitivity of plants to soil salinity depends on a number of factors such as the species, variety, rooting habits (Weil & Brady, 2017) and, potentially, on the soil's health, as there are studies suggesting that salt tolerance can be increased by soil microorganisms (Saghafi *et al.*, 2019). Depending on the species, plants have developed strategies in order to survive in saline environments (Weil & Brady, 2017). Table 1 gives some examples of EC_e threshold for crop growth without yield loss and the expected yield drop in % per dSm^{-1} increase in EC_e, according to Minhas *et al.* (2020).

Table 1: Salt tolerance at different horticultural crops according to Minhas *et al.* (2020)

Crop	EC_e threshold without yield loss [dSm^{-1}]	Decrease in yield above the threshold [% per dSm^{-1}]
	Sensitive crops	
Bean	1.0	19
Carrot	1.0	14
Strawberry	1.0	33
Onion	1.2	16
	Moderately sensitive	
Turnip	0.9	9
Radish	1.0	13
Lettuce	1.0	13
Pepper	2.0	14
Sweet potato	2.0	11
Broad bean	1.5-1.6	9.6
Corn	1.7	12
Potato	1.7	12
Cabbage	1.0-1.8	9.8-14
Celery	1.8-2.5	6.2-13.0
Spinach	2.0-3.2	7.6-16.0
Cucumber	1.1-2.5	7-13
Tomato	0.9-2.5	9.0-9.9
Broccoli	1.3-2.8	9.2-15.8
Squash (scallop)	3.2	16
	Moderately tolerant	
Beet	4.0	9
Squash (zucchini)	4.7-4.9	10.0

Spinach (*Spinacea oleracea* L.) is cultivated for its leaves, which are commercialized fresh, frozen or canned. It is an annual plant, with the vegetative phase occurring mostly in the form of a rosette (Almeida, 2006). As shown in table 1, spinach has moderate tolerance to soil salinity and does not show decrease in production with EC_e below 2 dSm^{-1}. After that, productivity decreases between 7.6 to 16% for each increased dSm^{-1}.

2.7 Modelling soil water content and soil salinity

Modelling the soil water content and salinity allows to predict the short- and long-term effects of irrigation water quality and irrigation schemes on crop yield, groundwater, and the environment, considering the specific soil-plant-climate conditions (Ramos *et al.*, 2011).

In order to model the soil-water-plant systems, it is necessary to handle a large body of input data, such as the soil physical properties, the root water uptake, evapotranspiration, irrigation, and precipitation. There are several tools which have been developed to support

modelling of these systems. Examples of such tools are water balance models such as: MOPECO-Salt and *SIMDualKc*. These models are limited to the assessment of evapotranspiration and yield reductions, however provide goods estimations of evaporation and transpiration needs for transient models. Transient models such as, SWAP, ENVIRO-GRO, SALTMED and HYDRUS-1D, allow considering and simulating temporal variations of certain parameters such as soil salinity, quality and volumes of irrigation water and specific physical and chemical properties of the soil profile (Ramos *et al.*, 2019). In the current work, *SIMDualKc* is used for estimation the crop evapotranspiration and *HYDRUS-1D* for modelling the water content and solutes in the soil.

2.7.1 *SIMDualKc*

SIMDualKc (Rosa *et al.*, 2012) is a software to estimate the crop evapotranspiration (ET_c) using the dual crop coefficient approach, as proposed by Allen *et al.* (1998) (Rosa *et al.*, 2012). *SIMDualKc* has been shown to be a powerful tool to calculate ET_c in greenhouses as well as in a soil salinity context (Liu *et al.*, 2022; Qiu *et al.*, 2015; Rosa *et al.*, 2016).

The crop evapotranspiration (ET_c) [mmd^{-1}] is calculated according to the equation:

$$ET_c = ET_o \times K_c \qquad \text{Equation 1}$$

where ET_o is the reference evapotranspiration for the study site and K_c is the crop coefficient.

ET_o is defined as the evapotranspiration from a grass surface with a crop height of 0.12 m, a fixed surface resistance of 70 sm^{-1} and an albedo of 0.23 (Allen *et al.*, 1998). Several methods have been developed for determination of ET_o. The FAO Penman-Monteith method was recommended as the standard method because it has been found to correctly predicting ET_o in a wide range of locations and climates and it is possible to apply in data-short situations (Allen *et al.*, 1998). Comparing ET_o measured inside the greenhouse with lysimeters and ET_o estimated from different methods, Fernández *et al.* (2010) and Fernández *et al.* (2011) conclude that the Hagreaves-Samani method is the most adequated to determine ET_o inside greenhouses and polytunnels due to its simplicity and accuracy comparable to other methods such as FAO Pennan-Monteith. In the Hargreaves-Samani, method ET_o is calculated according to the following equation (Hargreaves & Samani, 1985):

$$ETo = 0.0023 R_a \tau (T_{max} - T_{min})^{\frac{1}{2}} (T + 17.8) \qquad \text{Equation 2}$$

where *Ra* is a is the extra-terrestrial radiation, τ is transmissibility factor, T_{max} is the maximum temperature of day, T_{min} is the minimum temperature of day and T is the daily mean temperature.

K_c integrates the characteristics that distinguish the crop evapotranspiration from the reference grass surface. The calculation of ET_c according to equation 1 is called the single crop coefficient approach. Another approach is to split K_c into two factors that separately describe the evaporation and transpiration components, according to equation 3. This approach is called the dual crop coefficient approach. It is computationally more intensive than the single coefficient approach, and it is recommended for predicting the effects of specific wetting events (Allen *et al.*, 1998).

$$ET_c = ET_o \times (K_{cb} + K_e) \quad \text{Equation 3}$$

where K_{cb} is the basal crop coefficient and K_e is the soil evaporation coefficient. K_{cb} is defined as the ratio between ET_c/ET_o when the soil surface is dry but transpiration is occurring at a potential rate. K_{cb} is obtained from reference values by Allen *et al.* (1998) and adjusted according to equation 4:

$$K_{cb} = K_{cb(Tab)} + [0.04(u_2 - 2) - 0{,}004(RH_{min} - 45)](\frac{h_e}{3})^{0.3} \quad \text{Equation 4}$$

where $K_{cb(Tab)}$ is the reference values, u_2 is wind speed measured at 2 meters height, RH_{min} is minimum relative humidity and h_e is plant height.

K_e describes the evaporation component of ET_c and is calculated according to equation 5:

$$K_e = K_r\,(\mathrm{Kc}_{max} - \mathrm{K}_{cb}) \leq \mathrm{f}_{ew}\,\mathrm{Kc}_{max} \quad \text{Equation 5}$$

where K_r is dimensionless evaporation reduction coefficient, Kc_{max} is maximum value of K_c following rain or irrigation, and f_{ew} is fraction of the soil that is both exposed and wetted. Following rain or irrigation K_r is 1 and evaporation is maximal. As the soil surface dries, K_r becomes less than one and evaporation is reduced. K_r becomes zero when no water is left for evaporation in the upper soil layer. K_r is calculated by equation 6:

$$K_r = \frac{TEW - \mathrm{D}_{e,i-1}}{TEW - REW} \quad \text{Equation 6}$$

where *TEW* is total evaporable water, *REW* is the readily evaporable water and $D_{e,\,i-1}$ is the cumulative evaporative depletion of the previous day. This equation is used when *TEW* is lower than $D_{e,\,i-1}$, otherwise K_r is considered to be 1.

The Kc_{max} value is calculated according to the following equation:

$$Kc_{max} = \max(\{1{,}2 + [0{,}04(u_2 - 2) - 0{,}004(RH_{min} - 45)](\frac{h_e}{3})^{0.3}\}, (K_{cb} + 0.05)) \quad \text{Equation 7}$$

The equation 8 is used to calculate f_{ew}.

$$f_{ew} = \min(1 - f_c, f_w) \quad \text{Equation 8}$$

Where f_c is the fractional vegetation cover and f_w is fraction of soil surface wetted by irrigation or precipitation. Equations 8 shows that f_{ew} corresponds to the lowest value between the exposed soil fraction (1-f_c) and the wetted fraction.

Finally, transpiration (T_r) and evaporation (E) can be calculated using equations 9 and 10 respectively:

$$T_r = ET_O \times K_{cb} \quad \text{Equation 9}$$

$$E = ET_O \times K_e \quad \text{Equation 10}$$

The crop coefficients vary during crop development due to changes in ET_c during growth. The growth period can be divided into four distinct stages: initial, crop development, midseason, and late season, which are described by different values for the crop coefficients (Allen *et al.*, 1998). Plant transpiration and evaporation of soil are included on a single K_c coefficient. K_{cb}, is smaller than the K_c because only describes plant transpiration. The main difference between K_c and K_{cb} occurs in the initial growth stage when the plant is small and evapotranspiration is predominantly due to soil evaporation, given by K_e. Since canopies of horticultural crops mostly or totally cover the ground during the mid-season stage, soil evaporation beneath the canopy has less effect on crop evapotranspiration, and the K_{cb} value during this season will be approximately the same as K_c. Evaporation happens when we have a peak in K_e, generally after an irrigation or precipitation event, temporarily increasing evaporation. Over time, the layer dries and evaporation decreases, which leads to a decrease in K_e. Assuming that K_c is the sum of K_{cb} and K_e, we realize that when assuming the average, we are unable to describe the evaporation events as well as they are diluted in the average assumed by the single K_c. Figure 5 shows this effect.

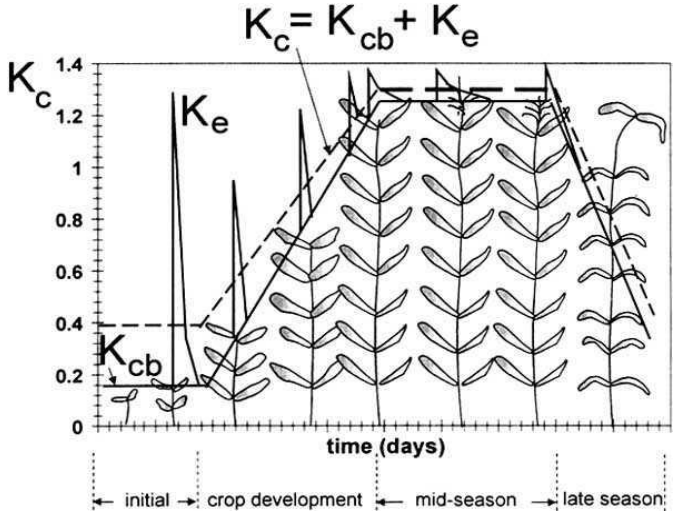

Figure 5: Crop coefficients curves: K_{cb} (thick line), K_e (thin line), and K_c curve (dashed line).
Source: (Allen et al., 1998)

2.7.2 *HYDRUS-1D*

Several modelling tools have been developed in the last decades to model the dynamics of water and solutes in porous media. One of these tools is the software package *HYDRUS-1D*, which allows one-dimensional modelling and simulation of water, heat, and solutes in variably saturated porous media (Šimůnek *et al.*, 2012). *HYDRUS-1D* has been shown to provide good simulations of water content and salt dynamics in the soil in semi-arid regions with drip irrigation (Er-Raki *et al.*, 2021; Gonçalves *et al.*, 2018; Kanzari *et al.*, 2018; Ramos, Liu, *et al.*, 2023; Zeng *et al.*, 2014).

HYDRUS-1D solves Richards' equation for water movement as well as the convection-dispersion equation for solute transport. Richards' equation (Richards, 1931) relates water content as a function of time to the capillary head, as shown in equation 11:

$$\frac{\partial \theta(h)}{\partial t} = \frac{\partial}{\partial z}\left[K(h)\left(\frac{\partial h}{\partial Z} + 1\right)\right] - S \qquad \text{Equation 11}$$

where θ is volumetric soil water content (volume of water/ volume of soil), h is the pressure head, t is time, z is the vertical coordinate positive upward, $K(h)$ is the unsaturated hydraulic conductivity function, and S is a sink term representing root water uptake. To solve this Richards' equation knowledge of the unsaturated soil hydraulic functions is required, namely: the soil water retention curve, $\theta(h)$, which describes the relationship between θ and the pressure head h, and the unsaturated hydraulic conductivity function, $K(h)$, which defines the hydraulic conductivity K as a function of h.

HYDRUS-1D includes five different models for description of the soil hydraulic functions. One of the dual-porosity models is the van Genuchten-Mualem (van Genuchten, 1980), which predicts the soil hydraulic functions from the soil water retention parameters, namely Θ_s, Θr, α, n, and K_s.

Θ_s is the saturation volumetric water content, Θ_r is the residual volumetric content, α and n parameters refer to adjustment parameters related to porosity, K_S is the saturated hydraulic conductivity.

The root water uptake (S) is calculated using the macroscopic approach introduced by Feddes (1982), as follow:

$$\mathrm{S}(\mathrm{h}, h_\phi, \mathrm{r}, \mathrm{z}, \mathrm{t}) = \mu(\mathrm{h}, h_\phi, \mathrm{r}, \mathrm{z}, \mathrm{t}) S_p(\mathrm{r}, \mathrm{z}, \mathrm{t}) = \mu(\mathrm{h}, h_\phi, \mathrm{r}, \mathrm{z}, \mathrm{t}) \beta(\mathrm{r}, \mathrm{z}, \mathrm{t}) T_p(\mathrm{t}) \mathrm{A}_t \qquad \text{Equation 12}$$

where $S(h,h\phi,r,z,t)$ and $S_p(r,z,t)$ are the actual and potential volumes of water extracted from a unit volume of soil (r,z) per a unit of time (t), respectively, $\mu(h,h\phi,r,z,t)$ is the root-water uptake water stress response function, a dimensionless function of the pressure head (h) and osmotic pressure ($h\phi$), which varies between 0 and 1, $\beta(r,z,t)$ is a normalized root density

distribution function, T_p is the potential transpiration rate and A_t is the area of the soil surface associated to transpiration.

Figure 6 shows the root water uptake water stress response function μ (h), as proposed by Feddes (1982). The stress function is zero above saturation (h1), an approximation of the "anaerobiosis point", and below the wilting point (h4), and is considered maximal between pressure heads h2 and h3.

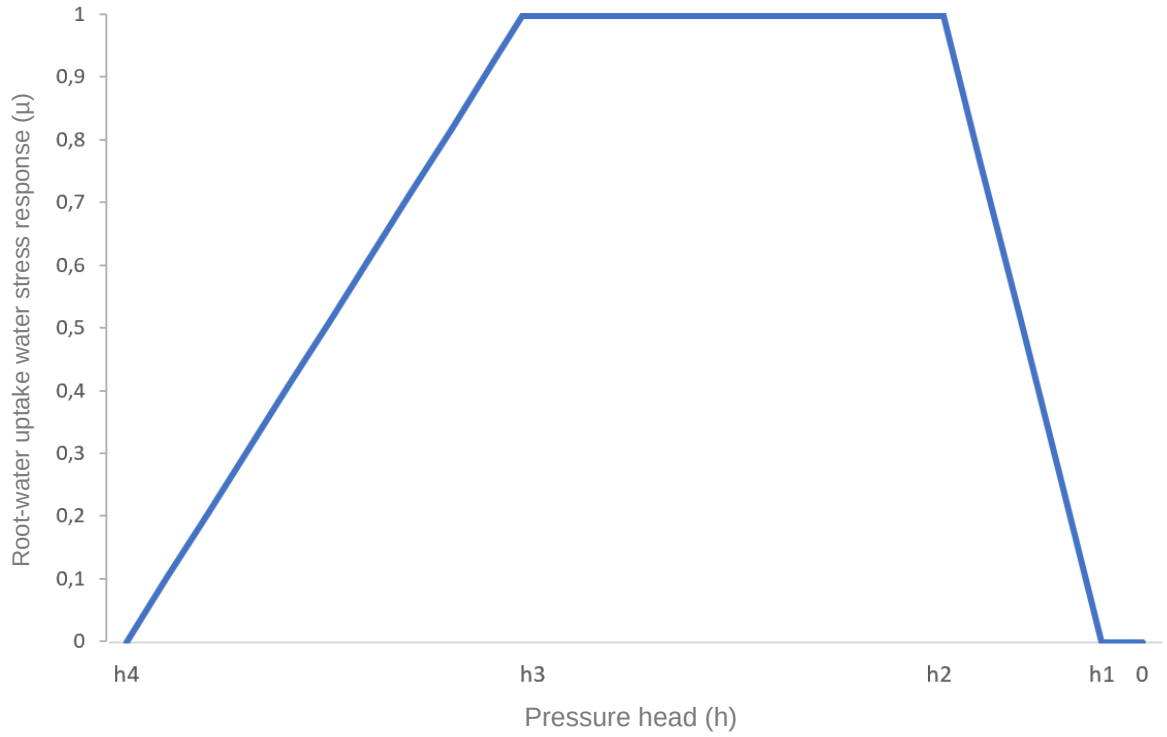

Figure 6: Root water uptake water stress response function α (h)

The *S* can be affected by water and salinity stresses. *HYDRUS-1D* also includes different approaches for modelling the salinity stress, such as the threshold-slope model by Maas (1984), where the root water uptake decreases according to a certain slope, when the salinity threshold is reached.

For the transport of solutes, *HYDRUS-1D* uses the partial differential equations governing one-dimensional solute transport under transient flow in a variably-saturated rigid porous medium equation, as follows:

$$\frac{\partial(\theta c)}{\partial t} + \rho\frac{\partial s}{\partial t} = \frac{\partial}{\partial z}\left(\theta D\frac{\partial c}{\partial z}\right) - \frac{\partial qc}{\partial z} - \phi \quad \text{Equation 13}$$

In equation 13, *c* is the solution concentration, ρ is the soil bulk density, *s* is the adsorbed concentration, *D* is the dispersion coefficient accounting for both molecular diffusion and hydrodynamic dispersion, θ is the volumetric water content, *q* is the volumetric fluid flux density evaluated using the Darcy–Buckingham law, and ϕ is a sink–source term that

accounts for various zero- and first-order decay or other reactions. In order to solve equation 13, the solute transport parameters are needed to estimate *s* and *D*, namely the tortuosity parameter in the conductivity function (I), longitudinal dispersivity, and molecular diffusion coefficient in free water.

In the current work, the solution concentration, *c*, refers to the amount of dissolved salts in the soil water, that is the electrical conductivity of the soil solution (EC_{sw}), used for modelling the soil salinity.

3. Material and Methods

The study presented in this thesis is part of a larger field experiment within the project *SoilSalAdapt*. As referred to introduction, in this project several field experiments where conducted with different crops and irrigation treatments. This thesis uses the data from the experiments performed with spinach using three different soils and one irrigation treatment. The experimental design and implementation of the experiment and the data collection were performed by the team at the University of Lincoln and were outside the scope of the work presented in this thesis.

3.1 Experimental Setup

This section, describes the experiment design carried out by the team of University of Lincoln, which design, implementation and data collection were outside the scope of the current work. The field experiment took place at Lincoln University in Lincoln, UK (N 53° 16' 6.841" W 0° 31' 24.697"). The experiment was carried out between June and September 2022. It was implemented by the project team at the University of Lincoln, which was also responsible for monitoring and data collection. Spinach was grown in large scale pots with 0.4 m length and 0.3 m diameter, with holes at the bottom, which allow for free water drainage, without fertilization. Pots were placed inside a polytunnel and were filled with three different soils (figure 7).

Figure 7: Experimental setup with the pots placed inside the polytunnel.

For each soil type, five pots were used as repetitions, of which three were chosen due to their similarities. All the pots were irrigated using a drip system and precipitation was simulated using a sprinkler. A number of five spinaches were seeded per pot. Because the spinach growth cycles were rather short, two growth cycles were carried out in order to achieve

a larger monitoring period. During the first cycle, spinaches were irrigated with non-saline water and, at the last 16 days of the second cycle, irrigation was made with 9 dSm^{-1} water. The choice to apply saline irrigation at the end of the second cycle intended to simulate the conditions that English farmers face at the end of the summer campaign, when the salinity of the available irrigation water raises The first growing cycle was 34 days long and the second was 36 days long. During the growing cycles, there was as an evaluation of the plants' health status and photos of the plants' growth were taken. Figure 8 shows a scheme of the experimental setup with the duration of each growing cycle, and the irrigation cycles.

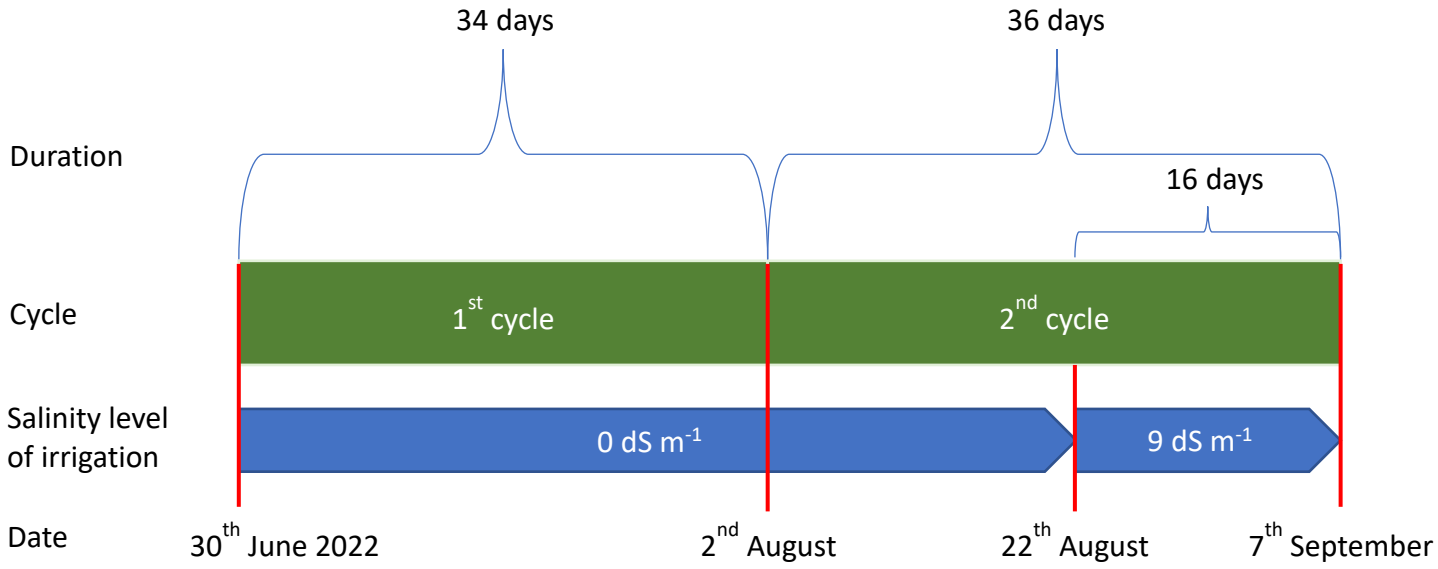

Figure 8: Scheme of experimental setup for the field experiment implemented in Lincoln, UK.

The soil volumetric water content (θ) and soil bulk electrical conductivity (EC_b) were monitored once a week, at the soil depths of 7,5 cm and 20 cm, using a time-domain reflectometer (Spectrum Fieldscout TDR350), TDR. It was necessary to obtain EC_{sw} from the measured EC_b, in order to model the solutes movement with *HYDRUS-1D*. The model proposed by Rhoades *et al.* (1976), as described and implemented by Kargas & Kerkides (2012) was used to obtain EC_{sw} from EC_b.

After the implementation of field experiment by the project partner, during the modelling task, it was noted that θ measurements were overestimated when EC_b was high. This is known to occur for TDR instruments as a result of the large dispersion of the electromagnetic wave at high *EC* (Peng *et al.*, 2022). In order to be able to use the data for this experiment, a correction of the TDR measurements was attempted. To make this correction, independent soil samples were collected and the water content was measured by TDR and determined using the gravimetric method. Subsequently, a regression analysis between the data measured by TDR and those obtained with the gravimetric method was carried out. Using this

regression a correction was made in soil water content , necessary for the modelling with HYDRUS-1D.

3.2 Soil properties

The experiment used three different soils which were collected in the East Midlands region in the UK. Two soils were originated from a coastal area in the county of Lincolnshire (sandy loams) and the third soil was collected in the county of Leicestershire (loam). The particle size distribution was determined using the pipette method and the Atterberg scale. Table 2 shows soil textural class, according to the diagram by Gomes & Silva (1962), the particle size distribution, and the bulk density for each soil type.

Table 2: Particle size distribution, bulk density and textural classes for soil types

Soil textural class	Coarse sand (200-2000 µm)	Fine sand (20-200 µm) [%]	Silt (2-20 µm)	Clay (<2 µm)	Bulk density [gcm^{-3}]
Sandy loam 1	57.98	25.01	5.41	11.6	1.4
Sandy loam 2	1.31	76.05	9.04	13.61	1.3
Loam	20.16	36.32	21.04	22.48	1.1

3.3 Input data for the *SIMDualKc*

The software *SIMDualKc*, described in the literature review, was used to estimate ET_c and its two processes, soil evaporation (E) and crop transpiration (T_r) under standard conditions, required by HYDRUS-1D, based on the dual crop coefficient on a daily period. The next sections describe how the input data necessary for the calculation of ET_c, E and T_r was obtained.

3.3.1 Estimation of ET_o

Estimation of ET_o is the start point for obtaining ET_c. ET_o was calculated according to the Hargreaves method (equation 2). R_a was computed daily as a function of the latitude of the experimental site (Allen *et al.*, 1998) using *STELLA* software (Liu *et al.*, 2003). τ was obtained by performing measurements of solar radiation inside and outside the polytunnel at three different times resulting in a transmissivity factor of 0.70, wich is the ratio between indoor and outdoor radiation. T_{max} and T_{min} were obtained from the temperature monitored inside the polytunnel. Figure 9 shows ET_o, T_{min} and T_{max} for the period of the field experiment.

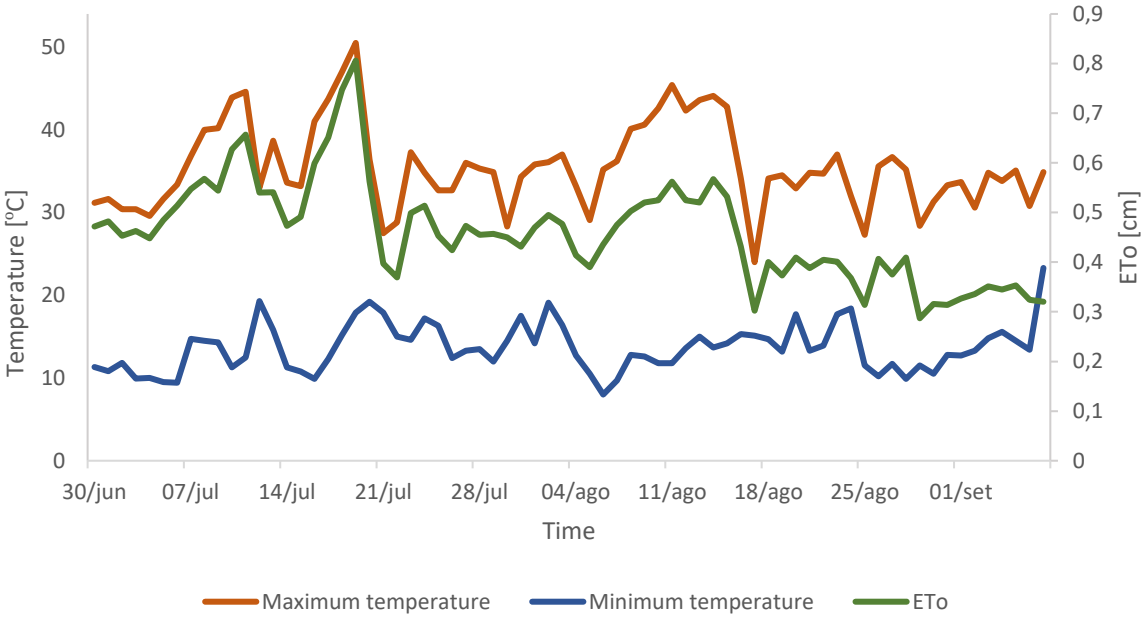

Figure 9: Measured T_{min} and T_{max} inside the polytunnel and ET_0 obtained with the Hagreaves-Samani equation

3.3.2 Crop data

In order to obtain the duration of the four growing stages, the total length of the spinach cycle, as presented by Allen *et al.* (1998), was used as reference, and the duration of each stage was obtained proportionally, for the two cycle lengths in our study (34 and 36 days). $K_{cb(Tab)}$ values for spinach were taken from Allen *et al.* (1998). The $K_{cb(Tab)}$ curve for the spinach with a full cycle of 36 days (second cycle) is shown in figure 10. The curve for first cycle is similar to the curve of second cycle differing in the duration of growing stages.

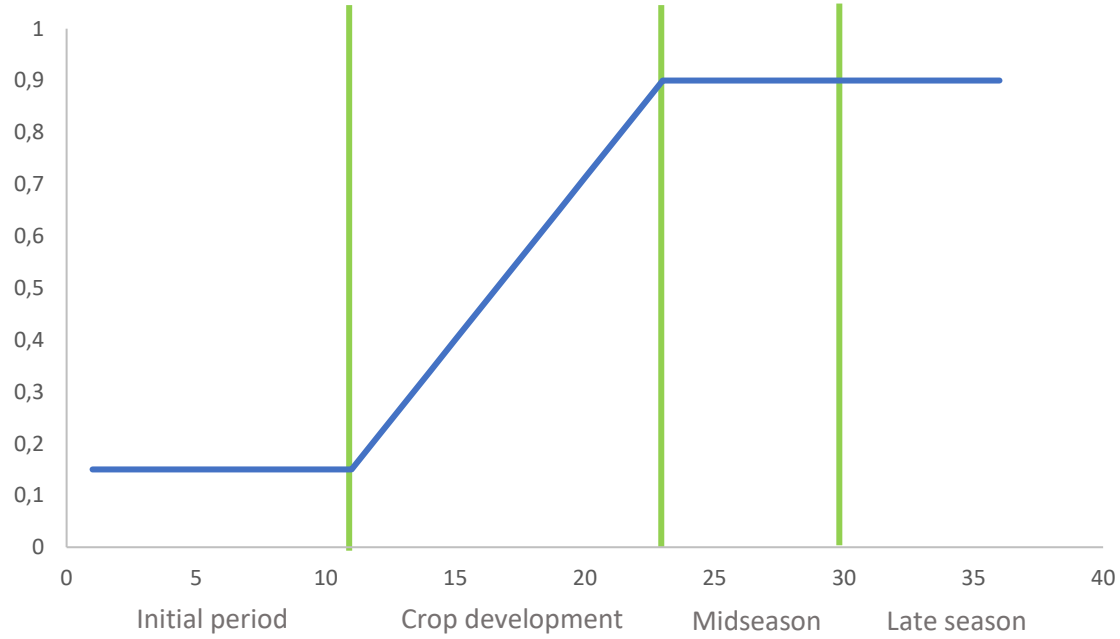

Figure 10: Reference basal crop coefficient curve ($K_{cb(Tab)}$) for spinach in the second with a growth cycle of the experiment (cycle length of 36 days).

By observing the photographic records, based on the maximum values of crop height and root length presented in Allen *et al.* (1998) and the measured plants height and root length of the harvest, an estimate was made of plant height for each stage, needed for equation 4 and 7 and root depth, used in *HYDRUS-1D*, as shown in table 3.

Table 3: Estimated growing stage length, root depth and plant height for spinach

	Growing stage length [days]		Root depth [m]	Plant height [m]
	1st cycle	**2nd cycle**		
Initial period	11	11	0	0
Crop development	11	12	0.2	0.07
Midseason	8	8	0.3	0.25
Late season	4	5	0.3	0.3

3.3.3 Wind velocity and Relative Humidity

In order to adjust the K_{cb} values to the site conditions according equation 4 and calculate Kc_{max} (equation 7), *SIMDualKc* uses wind speed and minimum relative humidity. The wind speed was obtained from a nearby meteorological station, assuming a reduction of 25% in wind speed inside the polytunnel. The obtained values of wind speed inside of polytunnel are similar to those described by Teitel et. al (2008). The minimum relative humidity was obtained from the measurements inside the polytunnel. Figure 11 shows the minimum relative humidity measured inside the polytunnel and the wind speed considered inside the polytunnel.

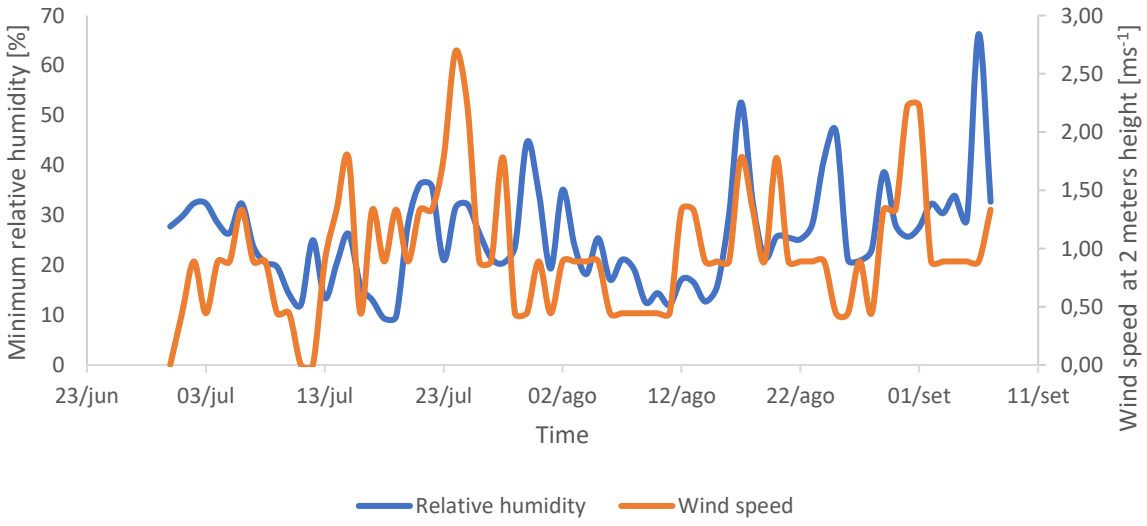

Figure 11: Relative humidity and wind speed inside the polytunnel

3.3.4 Precipitation and Irrigation

Precipitation was simulated using a sprinkler placed in each pot, distributing water with fine pluviometry at a 45º angle. The volumes and distribution of precipitation were based on historical precipitation series for the area of the experimental site and the water used to simulate precipitation had *EC* of 0 dSm^{-1}. Irrigation occurred through a drip system with 5 drippers arranged in a circle in the middle of the pot, as shown in figure 12.

Figure 12: Pot irrigation scheme, where the purple stick is the sprinkler and the white ring the drip system

Irrigation water had *EC* of 0 dSm^{-1} in the beginning of the growth cycles and, in the last 16 days of second cycle (from the 22th august), water had an *EC* of 9 dSm^{-1}, in order to simulate the irrigation water conductivity conditions that English farmers face in the summer. Irrigation amounts were determined by the Lincoln University team empirically, considering the particular experience of the crop's water requirements. Figure 13 shows precipitation and irrigation amounts, calculated using the duration and flow rate of emitters, divided by the area of the pot. These amounts were used as input data in both *HYDRUS-1D* and *SIMDualKc*, in the last one to calculate $D_{e,\,i-1}$.

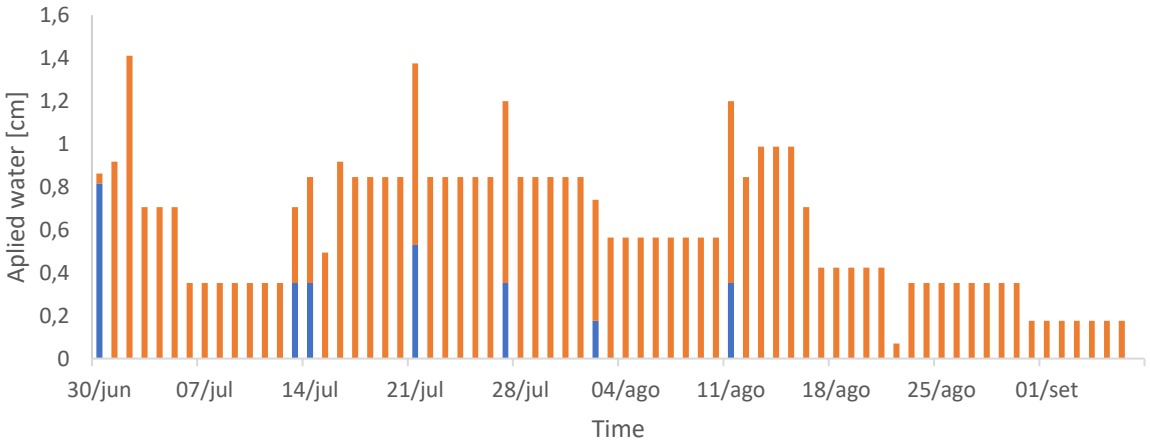

Figure 13: Precipitation and irrigation water applied to the experimental pots

3.3.5 Soil data

Using a default value of 10 cm for the evaporative layer, as suggested by Allen *et al.* (1998), pedotransfer functions inbuild in *SIMDualKc* were used to estimate *TEW* and *REW*, in order to calculate K_r, according the equation 6. In table 4, the estimates made by *SIMDualKc* of *TEW* and *REW* as show:

Table 4: Estimates for TEW and REW obtained from SIMDualKc

	Sandy Loam 1	Sandy Loam 2	Loam
***TEW* [mm]**	21	29	34
***REW* [mm]**	8	9	10

3.3.6 Fractional vegetation cover

To estimate the fractional vegetation cover (f_c), necessary for the equation 8, the application *Canopeo* (Patrignani & Ochsner, 2015) was used. This application is based on the ratio of red to green (R/G) and blue to green (B/G) colours in each pixel, as well as an excess green index (2G-R-B). The R/G and B/G ratios must be lower than 0.95 (P_1 and P_2) and the excess green index must be higher than 20 (P_3). These three conditions must be met in order to classify the pixel as green:

$$R/G < P_1 \text{ and } B/G < P_2 \text{ and } 2G\text{-}R\text{-}B > P_3$$

Based on the analysis of all pixels of the image, f_c is calculated with a with average error of less than 1% (Patrignani & Ochsner, 2015). The software gives faster estimates of the fraction of ground cover than other software packages, such as *SamplePoint* version 1.56 and *SigmaScan Pro 5* (González-Esquiva *et al.*, 2017; Patrignani & Ochsner, 2015).

A pot picture processing by *Canopeo* to estimate the fraction of soil cover, as show in figure 14.

Figure 14: Pot picture processed by Canopeo. In this example shows a f_c estimative of 56,9 %

The f_c was used in *SIMDualKc* with fraction of soil surface wetted (f_w) for calculating the f_{ew} (equation 8), which is needed for obtaining K_e (equation 5). Since the system is a dripper, installed in pots (section 3.3.4), it was assumed that the f_w is 0.9. Table 5 shows f_c obtained with *Canopeo*.

Table 5: Estimates of fc in different dates for each soil type, obtained from Canopeo

	f_c [%]		
Date	Sandy Loam 1	Sandy Loam 2	Loam
First cycle			
12/jul	1.40	3.83	1.81
2/ago	75.45	95.10	86.55
Second cycle			
16/ago	0.83	1.09	0.62
26/ago	15.66	19.98	13.12
5/set	56.92	77.47	70.75

3.4 Input data for the *HYDRUS-1D*

HYDRUS-1D software was used to model soil water content and soil salinity, using the estimates of soil evaporation and crop transpiration under standard conditions made by *SIMDualKc*. The remaining inputs and assumptions are described in the following sections.

3.4.1 Boundary conditions

Atmospheric and free drainage conditions were defined as boundary conditions at the surface and bottom of the pot. The atmospheric boundary conditions were E and T_r, obtained as outputs of the *SIMDualKc*, and the irrigation and precipitation amounts (section 2.3.4). Regarding the solutes, a concentration flux boundary condition was defined at the top and a zero concentration gradient condition at the bottom, because solutes were applied in irrigation at a constant concentration. The considered fluxes at the boundaries of the system are shown in figure 15.

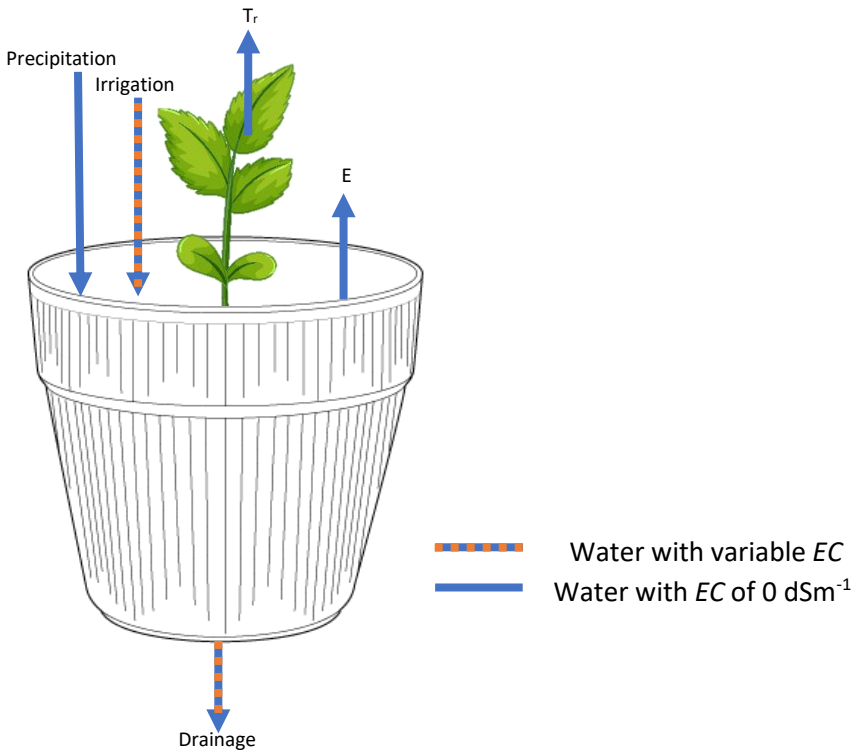

Figure 15: Fluxes and boundaries of the system considered at HYDRUS-1D. Inflows was precipitation and irrigation and outflows was transpiration (Tr), evaporation and drainage

3.4.2 Soil hydraulic parameters

The van Genutchen model (van Genuchten, 1980) was used to estimate the soil hydraulic functions. The van Genuchten parameters required by the model were obtained from the particle size distribution and bulk density, using the pedo-transfer functions described by Ramos *et al.* (2014). Table 6 shows the van Genuchten parameters obtained with the pedo-transfer functions. The hydraulic parameters for the three soils were finetuned during the calibration of the models.

Table 6: van Genuchten parmeters obtained with the pedo-transfer functions by Ramos *et al.* (2014)

	θ_r	θ_s	α	n	Ks	l
	[cm^3cm^{-3}]	[cm^3cm^{-3}]	[cm^{-1}]		[cm day^{-1}]	
Sandy loam 1	0.044	0.392	0.087	1.35	115.6	-2.6
Sandy loam 2	0.039	0.386	0.043	1.29	24.0	-2.6
Loam	0.062	0.421	0.044	1.20	37.1	-5.6

3.4.3 Solute transport parameters

The solute transport parameters, longitudinal dispersivity, and diffusivity, were considered the same for all soil types. Diffusivity was considered 2, a typical value for setups with saline water. The longitudinal dispersivity was assumed as 3, corresponding to one-tenth of the transport distance, being a good approximation according to Mallants *et al.* (2011).

3.4.4 Root water uptake

The parameters used in the Feddes model (h1, h2, h3l, h3h, h4), as described in section 2.7.2, for determination of α were those proposed to spinach by Sao *et al.* (2021) (table 7). Regarding the parameters for saline stress, they were 4 dSm^{-1} of EC_{sw} for threshold and 3,8 for slope, values indicated by Maas (1984), for spinach.

Table 7: Spinach parameters used in Feddes model for calculation root water uptake, obtained from (Sao *et al.*, 2021)

Parameter	Value [cm]
h1	-10
h2	-25
h3l	-50
h3h	-50
h4	-1000

3.4.5 Initial conditions

The initial conditions for θ and EC_{sw} were necessary to start modelling these variables. As the first TDR measurement was made on July 5th, it was considered as the first day of the simulation, and those were defined as initial conditions. In order to obtain more accurate models and as the TDR measurements were carried out at two depths, two soil layers were defined, from 0 to 15 cm and from 15 to 30 cm. In both layers, the initial values for θ and EC_{sw} are shown in table 8.

Table 8: HYDRUS-1D modelling initial conditions for θ and EC_{sw}

	θ [cm^3cm^{-3}]		EC_{sw} [dSm^{-1}]	
	Top	Bottom	Top	Bottom
Sandy loam 1	0.103	0.145	1.29	1.66
Sandy loam 2	0.172	0.176	2.5	3.22
Loam	0.220	0.217	1.94	1.47

4. Results and discussion

4.1 Correction of soil water content measurements

As indicated in section 3.1, during the experiment it was noted that θ measurements by the TDR were overestimated for higher *EC* values. This is known to occur for TDR instruments as a result of the large dispersion of the electromagnetic wave at high *EC*. To correct the θ measurements, a regression was made between TDR measurements and θ determined with the gravimetric method.

The logarithmic regression resulted in the lowest error. For each type of soil, a regression was carried out. Figures 16, 17, and 18 show the regressions, equations and respective determination coefficients for sandy loam 1, sandy loam 2 and, loam, respectively. The determination coefficients (R^2) were over 0.76 for all soil types, reflecting a high correlation between the θ determined with gravimetric method.

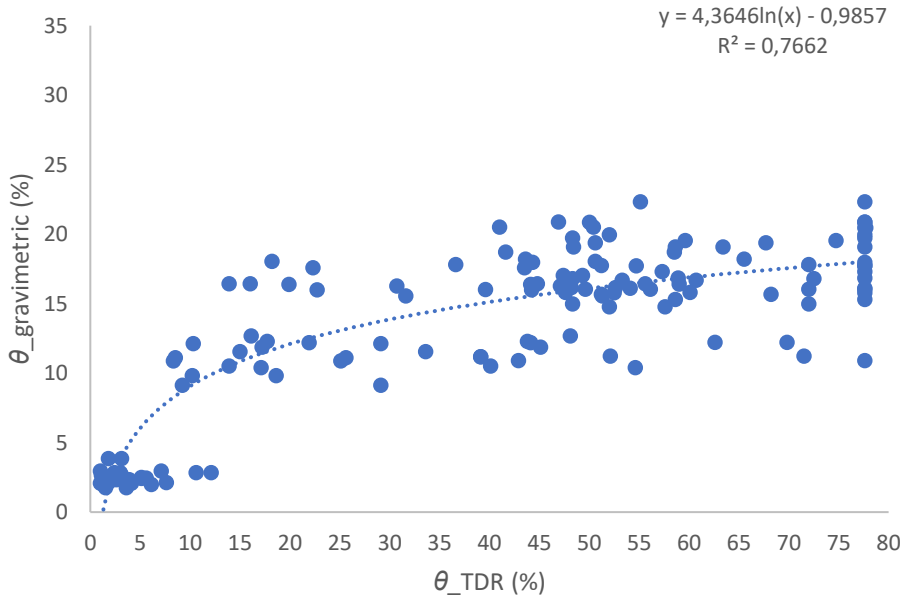

Figure 16: Logarithmic regression between θ measured with TDR and with the gravimetric method for sandy loam 1

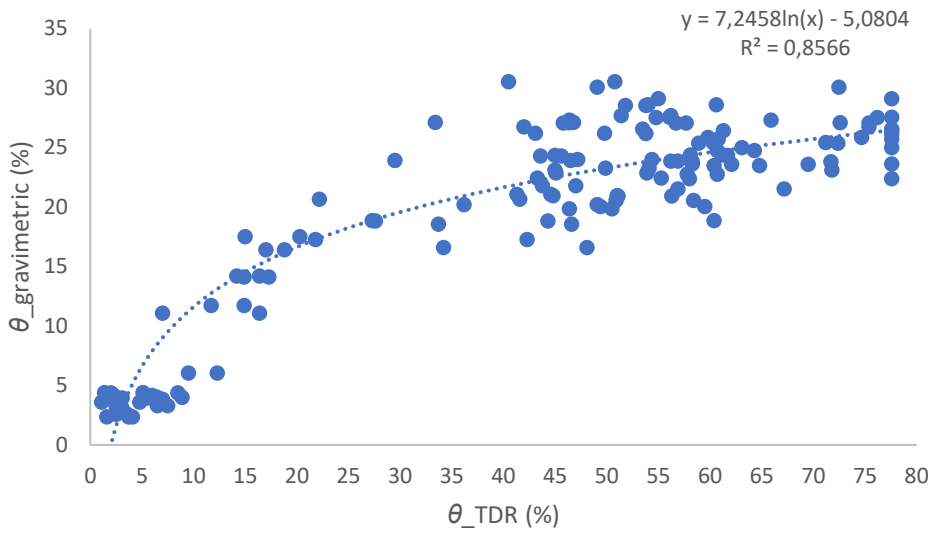

Figure 17: Logarithmic regression between θ measured with TDR and with the gravimetric method for sandy loam 2

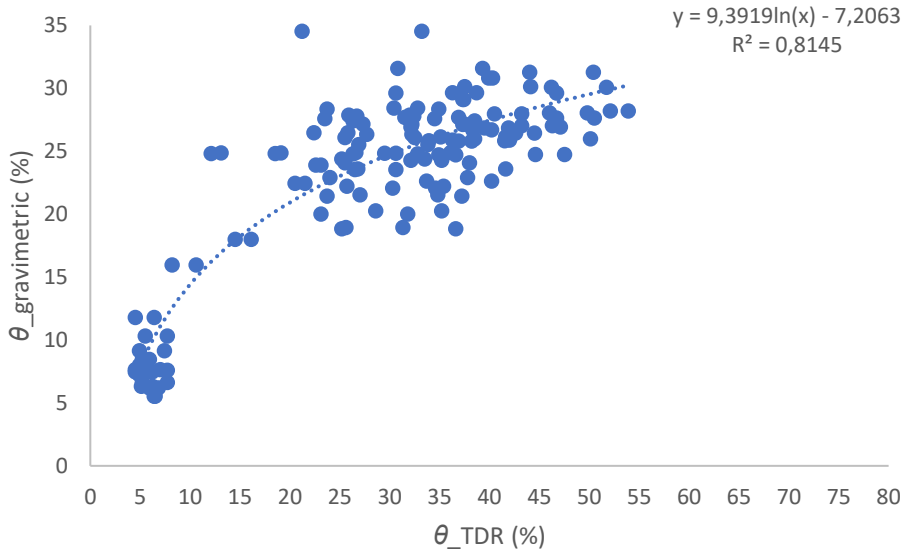

Figure 18: Logarithmic regression between θ measured with TDR and with the gravimetric method for loam

It is important to note, that with increasing salinity the error tended to be greater. At lower salinities, the TDR was accurate, therefore the data correction was made when EC_b (bulk electrical conductivity) was greater than 0.02 dSm^{-1}. With this condition the achieved error was smaller. Table 9 shows the root mean square error (*RMSE*) between the θ determined by the

gravimetric method and 1) the TDR; 2) the corrected TDR measurements. The *RMSE* is considerably lower when using the corrected TDR values. Bittelli *et al.* (2008) presented a more complex method for correction of the TDR θ measurements, which included subtracting the dielectric losses from the dielectric permittivity. This authors achieved a *RMSE* between 0.03 and 0.05 cm^3cm^{-3}, which points out to a good correction ability of the logarithmic regression.

Table 9: RMSE between the θ determined by the gravimetric method and the TDR measurements (1st column) and RMSE between the θ determined by the gravimetric method corrected TDR (2nd column).

	θ _gravimetric vs. θ _tdr [cm^3cm^{-3}	**θ _gravimetric vs. θ _tdrcorrected [cm^3cm^{-3}]**
Sandy loam 1	0.343	0.028
Sandy loam 2	0.286	0.029
Loam	0.101	0.033

4.2 Evaporation and transpiration

Evaporation and transpiration for the three soil types under standard conditions, i.e. in the absence of water and saline stress, were obtained by *SIMDualKc*. Figure 19 show us the K_{cb} and K_e used to calculate evaporation and transpiration according to equations 9 and 10. In attachments, this values are show in table 12.

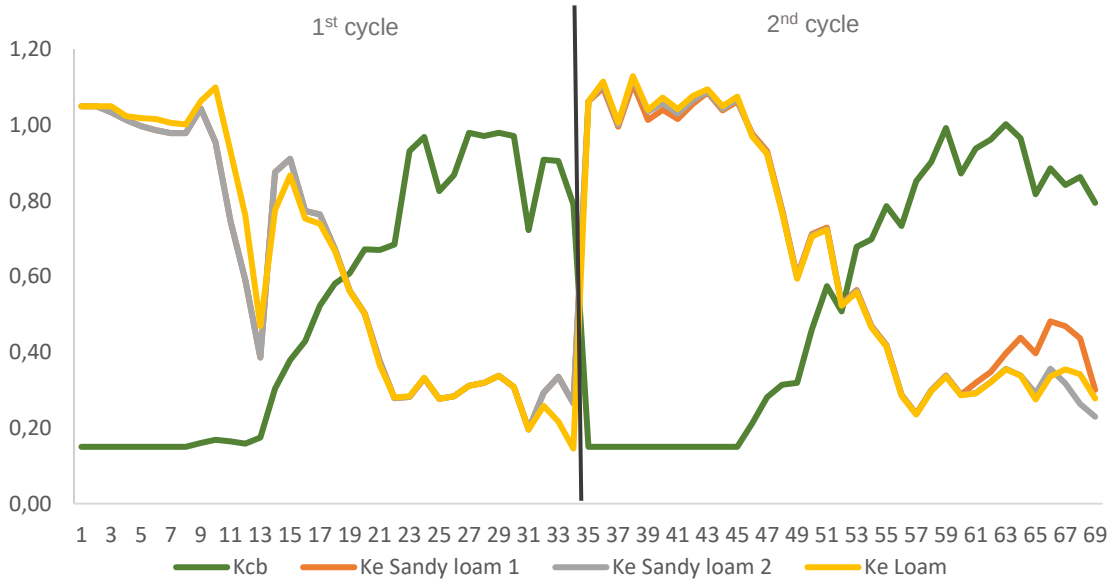

Figure 1919: Kcb and Ke coefficients for each day and for three soil types

Figures 21, 21, and 22 present the E, T_r, and ET_c in left axis and the irrigation and precipitation on right axis for sandy loam 1, sandy loam 2, and loam soils, respectively.

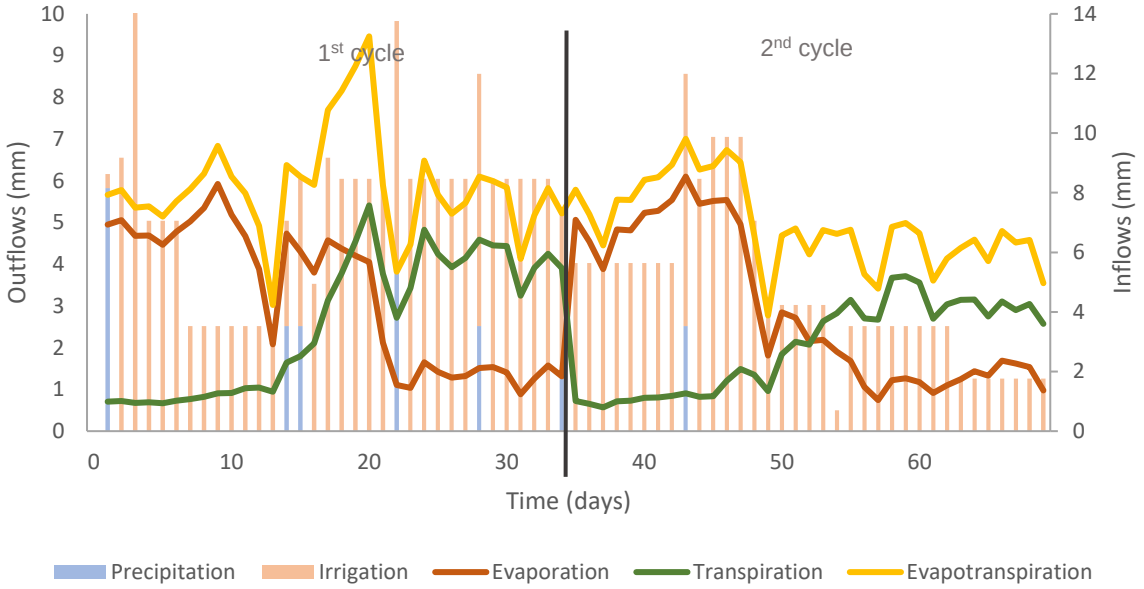

Figure 20: Evaporation, transpiration and evapotranspiration in left axis and precipitation and irrigation on right axis for sandy loam 1

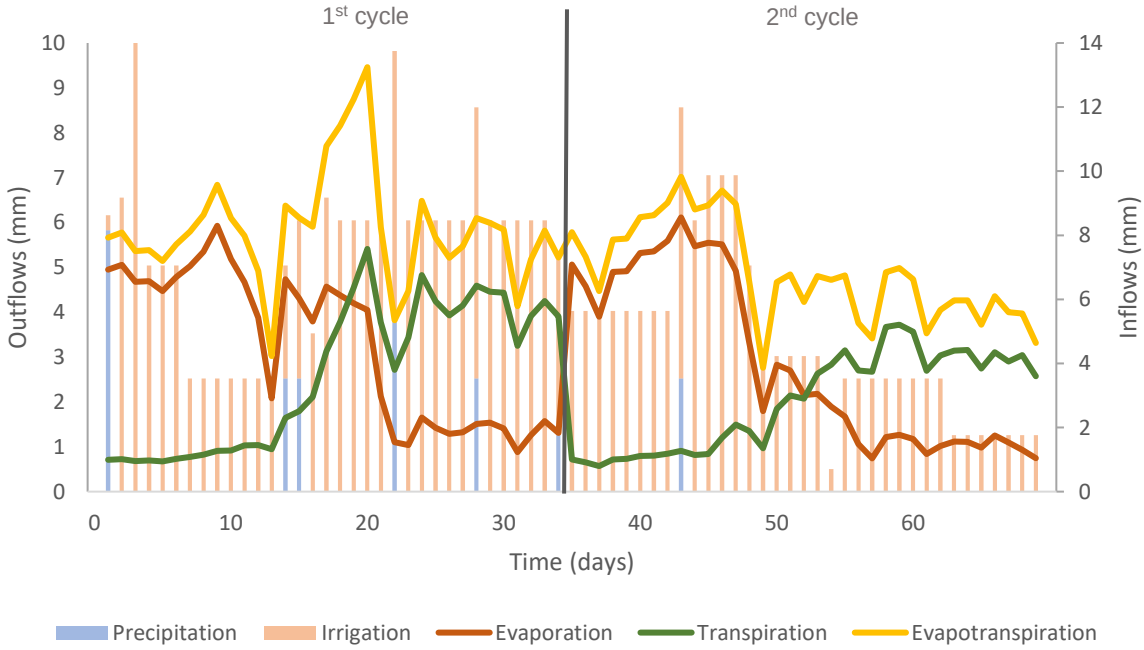

Figure 201: Evaporation, transpiration and evapotranspiration in left axis and precipitation and irrigation on right axis for sandy loam 2

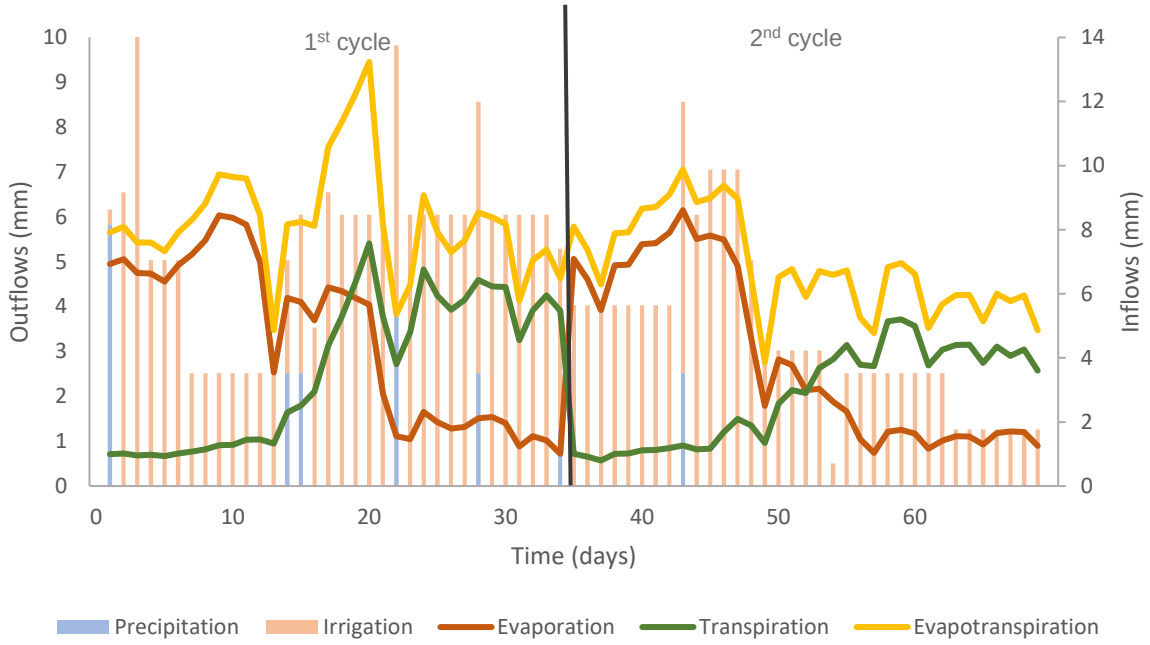

Figure 212: Evaporation, transpiration and evapotranspiration in left axis and precipitation and irrigation on right axis for loam

Differences during the growth cycle in evaporation, present in all soil types, are due to differences in the f_c, with evaporation being higher when the f_c is smaller, since the portion of the soil exposed to solar radiation is inversely proportional to the f_c. With the development of spinach, the f_c increases and therefore evaporation decreases. When spinach is harvested and the 2nd cycle starts (day 35), high evaporation occurs because f_c is zero. Comparing evaporation in the three soil types, loamy soil has slightly higher evaporation at the beginning of the first cycle. However, evaporation is quite similar in the three soils. At the end of the second cycle, when a 9 dSm^{-1} irrigation was applied, evaporations differed slightly depending on the type of soil, since the soils hydraulic properties' of the soil are different, giving different *TEW* and *REW*.

Transpiration under standard conditions is the same in the three soil types because K_{cb} does not vary depending on soil type, varying during the growing cycle in the same manner for all three soils.

4.3 Model calibration

HYDRUS-1D considers saline and water stress, making corresponding corrections to root water uptake, allowing for better adjustment of θ and EC_{sw}. In order to calibrate the model, the initial soil hydraulic parameters were fitted using the inverse modelling tool in *HYDRUS-1D*. The soil hydraulic parameters obtained after calibration are presented in table 10.

Table 10: Fitted van Genucthen parameters

		Top layer						Bottom layer					
		Θr	Θs	α	n	Ks	l	Θr	Θs	α	n	Ks	l
		[cm^3cm^{-3}]	[cm^3cm^{-3}]	[cm^{-1}]		[$cmday^{-1}$]		[cm^3cm^{-3}]	[cm^3cm^{-3}]	[cm^{-1}]		[$cmday^{-1}$]	
Sandy loam 1	Before	0.044	0.392	0.09	1.35	115.60	-2.6	0.044	0.392	0.09	1.35	115.60	-2.6
	After	0.044	0.393	0.04	1.60	250.00	-2.6	0.044	0.393	0.03	1.45	400.00	-2.7
Sandy loam 2	Before	0.039	0.386	0.04	1.29	24.00	-2.6	0.039	0.386	0.04	1.29	24.00	-2.6
	After	0.039	0.360	0.05	1.52	350.00	-2.6	0.039	0.360	0.09	1.45	200.00	-2.6
Loam	Before	0.062	0.421	0.04	1.20	37.10	-5.6	0.062	0.421	0.04	1.20	37.10	-5.6
	After	0.063	0.420	0.06	1.35	40.00	-3.0	0.063	0.421	0.04	1.45	55.00	-3.5

4.4 Soil water content and EC_{sw} modelling

This section presents the modelling of θ and soil salinity (EC_{sw}), considering that the first day of modelling corresponds to day 6 of the growing cycle. The beginning of the second cycle corresponds to day 29 in the model. Irrigation with an *EC* of 9 dSm^{-1} occurs a day 48 in the model.

The soil modelling of θ is shown in figures 24, 25, and 26 for the three soil types.

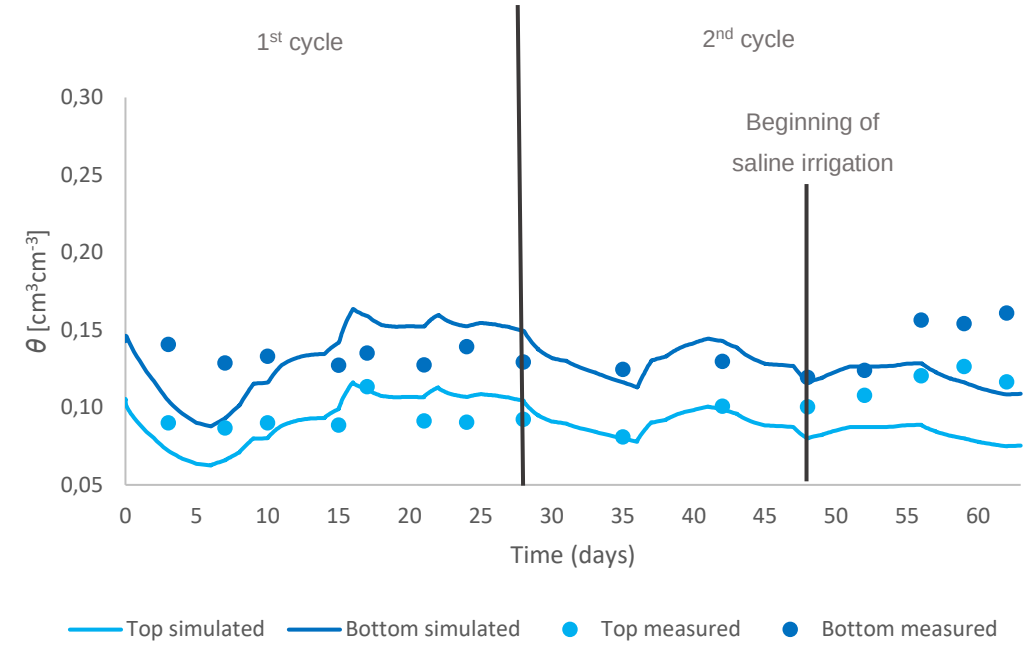

Figure 223: θ modelled (line) and θ observed (points) in sandy loam 1

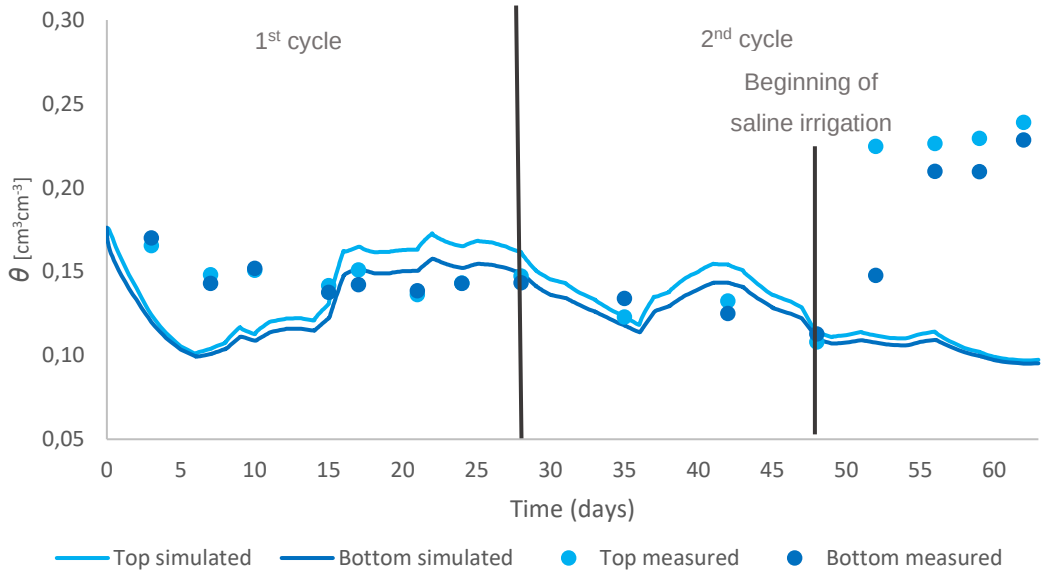

Figure 24: θ modelled (line) and θ observed (points) in sandy loam 2

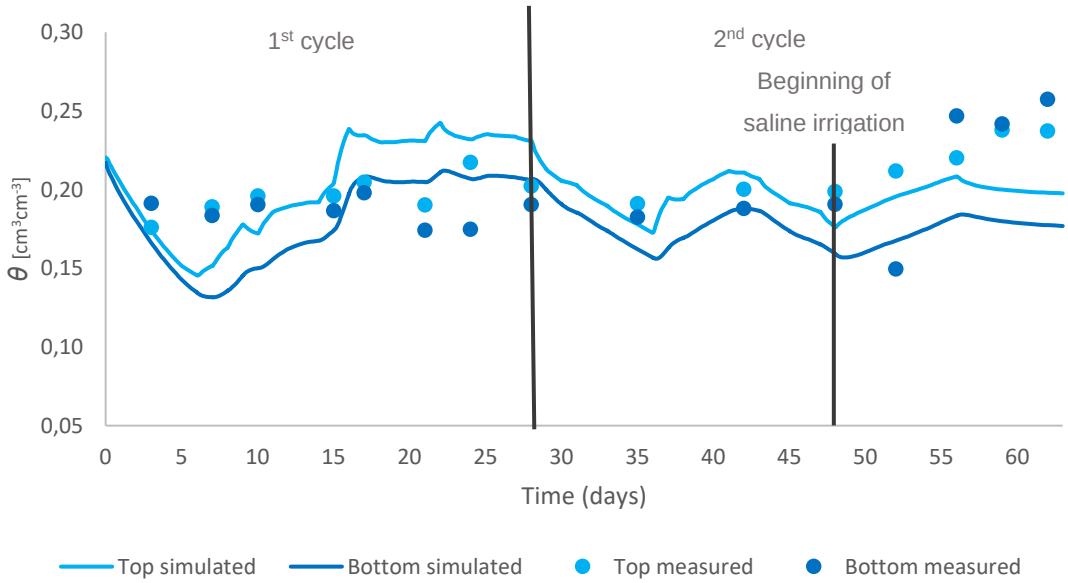

Figure 25: θ modelled (line) and θ observed (points) in loam

In the sandy loam 1 soil (figure 23), the deeper layer has higher θ than the top layer. In the first cycle, the modelled values are relatively close to the observed values. At the end of the second growing cycle, when the 9 dSm^{-1} irrigation is applied, the modelled θ is underestimated when compared to the observed data. The sandy loam 2 soil (figure 24) shows similar θ values at both depths. The modelling of the first cycle is well adjusted with observed values. Regarding the second cycle, the modelled θ is largely underestimated from day 50 onwards. Considering the loamy soil (figure 25), the modelling of θ is well adjusted for both depths, in the first cycle and at the beginning of the second cycle. At the end of the second cycle, there is again an underestimation of θ at both depths.

Since θ measurement error increases with salinity, even when applying a correction, there is an error in observed data associated with high salinity levels. Once the irrigation of 9 dSm^{-1} is applied, the salinity increases and results in larger measurement errors in θ. The modelling shows a tendency for the θ to increase, except in sandy loam 2 soil at the end of the second cycle, that has a trend contrary to what is measured.

The EC_{sw} modelling is shown in figures 26, 27, and 28 for the sandy loam 1, sandy loam 2 and loam soils, respectively.

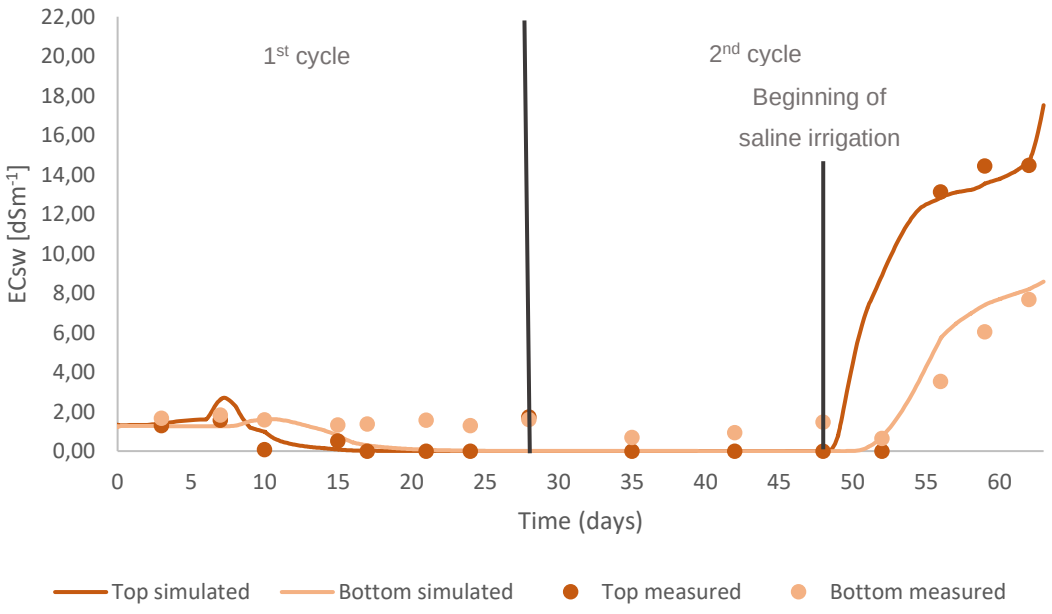

Figure 26: EC_{sw} modelled (line) and EC_{sw} observed (points) in sandy loam 1

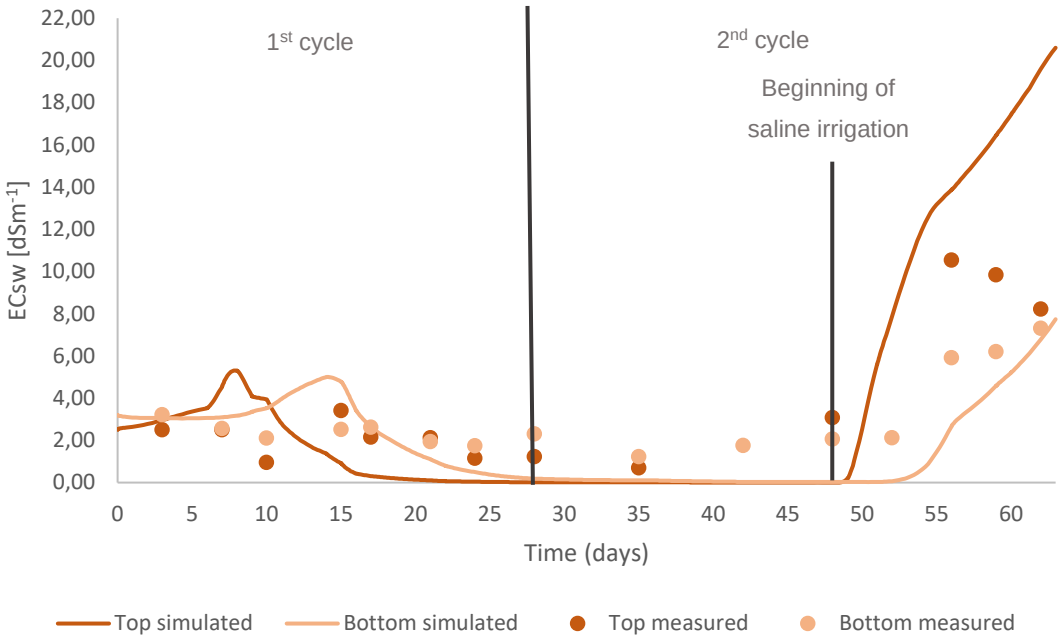

Figure 2723: EC_{sw} modelled (line) and EC_{sw} observed (points) in sandy loam 2

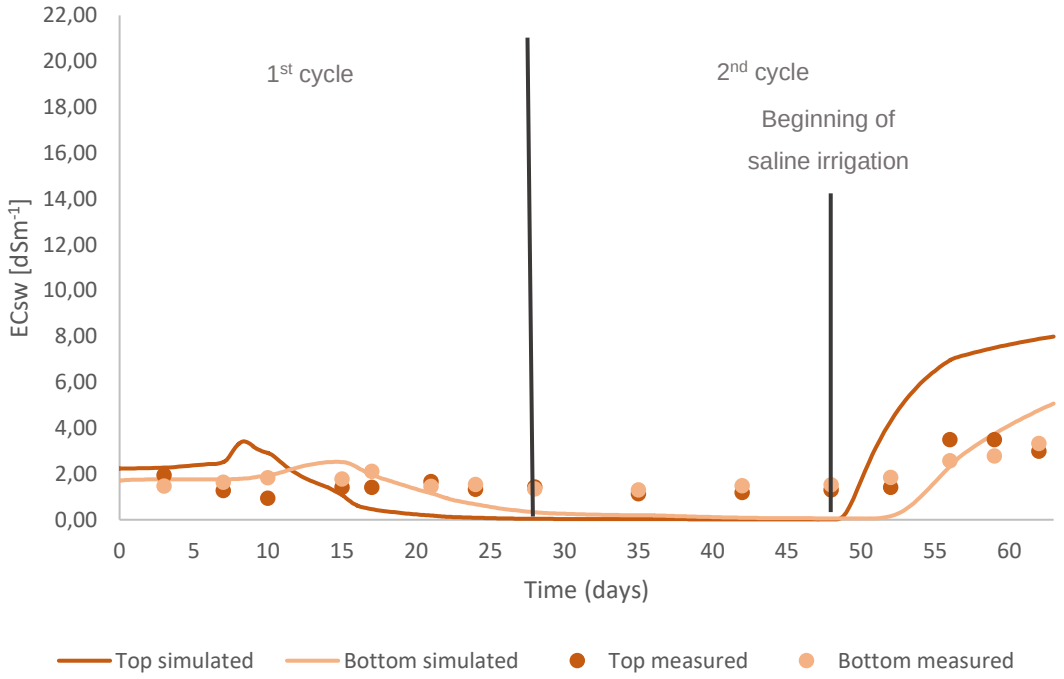

Figure28: EC_{sw} modelled (line) and EC_{sw} observed (points) in loam

In the case of sandy loam 1 soil, the observed and modelled values are very close, as shown in figure 25. In figure 26 and 27 the EC_{sw} observed and modelled shows some differences at the end of the second cycle, after the 9 dSm^{-1} irrigation was applied.

Since the θ simulation is not well adjusted at the end of the second cycle, and since the EC_{sw} depends on the θ, the EC_{sw} simulation will also show a deviation from reality. A greater error in θ gives, consequently, a greater error in EC_{sw}. However, the trend of increasing θ is

simulated. The θ is lower in sandy loam soils and higher in loam, which will also influence EC_{sw}, being lower in loam and higher in the others.

To evaluate the modelling accuracy, the *RMSE* for θ and EC_{sw} was calculated, for each growing cycle and the total length of experiment, and the results are shown in table 11.

Table 11: RMSE of θ and EC_{sw} models. RMSE are given for the first cycle, second cycle and total length of the trial

	Sandy loam 1			Sandy loam 2			Loam		
	1st cycle	2nd cycle	Total	1st cycle	2nd cycle	Total	1st cycle	2nd cycle	Total
θ [cm^3cm^{-3}]	0.020	0.027	0.024	0.029	0.081	0.063	0.029	0.036	0.033
EC_{sw} [dSm^{-1}]	0.915	2.445	1.861	1.655	4.244	3.312	0.960	2.217	1.736

As expected from the analysis of figures 23 to 28, the *RMSE* is lower for the first cycle when comparing with the second cycle. Considering the *RMSE* of θ and EC_{sw} for the total period, they were rather low in the case of sandy loam 1 and loam soil. In the case of sandy loam 2 soil, the relatively high *RMSE* is mainly due to the differences between observed and modelled values at the end of the second growth cycle, which were relatively larger in the case of sandy loam 2 soil (figure 24 and figure 27). The low *RMSE* values indicate that estimation errors are small. The ranges obtained are comparable with results from other *HYDRUS-1D* modelling of soil in lysimeters where *RMSE* in the range of 0.01 to 0.03 cm^3cm^{-3} for θ and 0.5-2.3 dSm^{-1} for EC_{sw} were achieved (Ramos, Darouich, *et al.*, 2023; Ramos, Liu, *et al.*, 2023).

4.4 Root water uptake and drainage

Root water uptake and drainage are obtained as output from the *HYDRUS-1D* models, allowing conclusions to be made about the θ and EC_{sw} models. Potential root water uptake refers to the water extracted by the roots for transpiration without stress, and actual root water uptake refers to transpiration with hydric and saline stress. The first day of modelling corresponds to day 6 of the growing cycle. The beginning of the second cycle corresponds to day 29 in the model. Irrigation with 9 dSm^{-1} is applied on day 48 in the model. Figure 29, 30 and 31 shows the variation in potential and actual root water uptake during the two cycles in sandy loam 1, sandy loam 2, and loam soils, respectively.

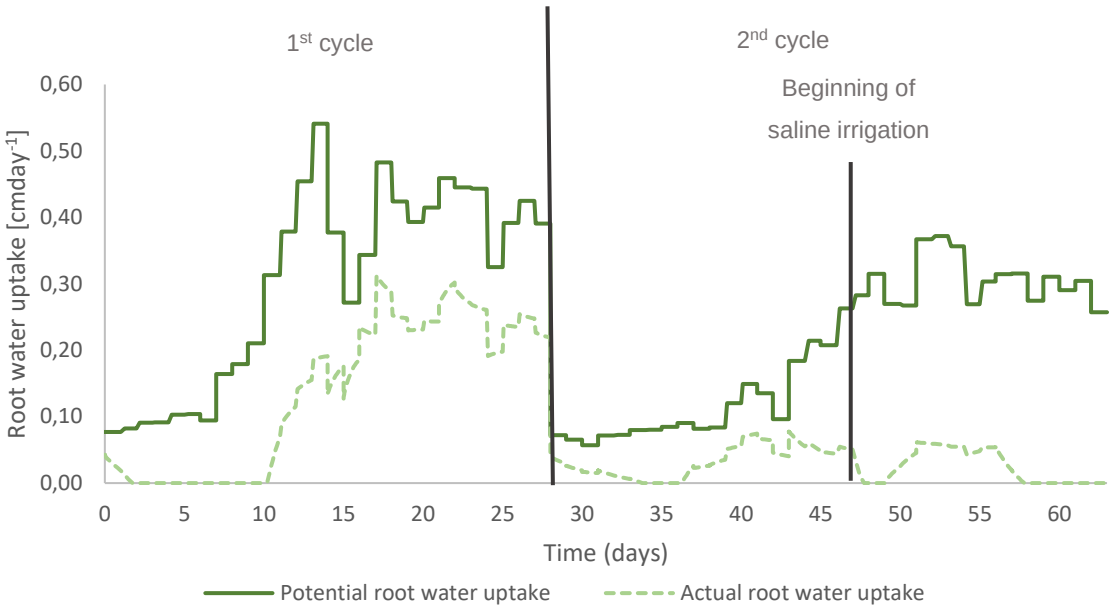

Figure 29: Potential and actual root water uptake in sandy loam 1

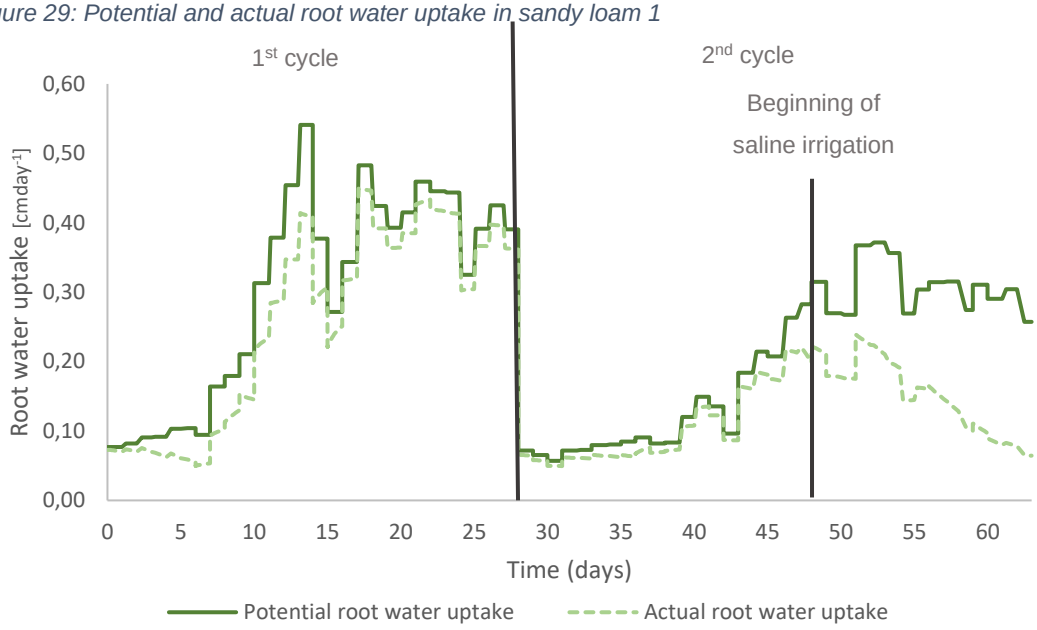

Figure 30: Potential and actual root water uptake in sandy loam 2

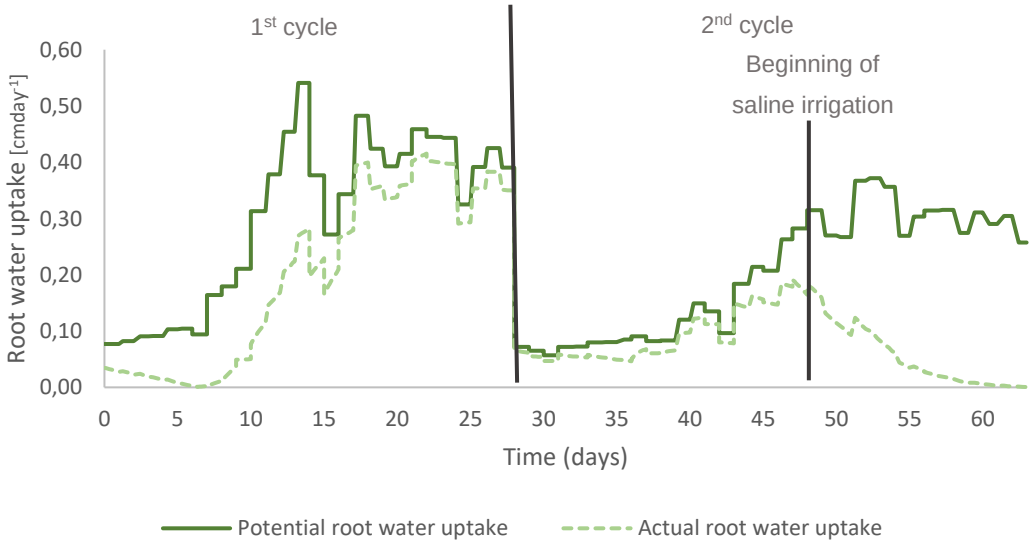

Figure 241: Potential and actual root water uptake in loam

The difference between potential and actual root water uptake are result of stresses reducing the ability of the crops to extract water from the soil, which can be due to water and salinity stresses. There is a larger difference between the potential and the actual root water uptake in sandy loam 1 than in other soils. This results from water stress, since in the first cycle, when there is no salinity, there is a considerable difference in root water uptake. The difference in water stress between soil types is due to the soils' hydraulic properties. However, saline stress is also evident in all soil types, since when an irrigation of 9 dsm^{-1} is applied, the actual root water uptake decreases.

Figures 32 shows the drainage in the three soil types.

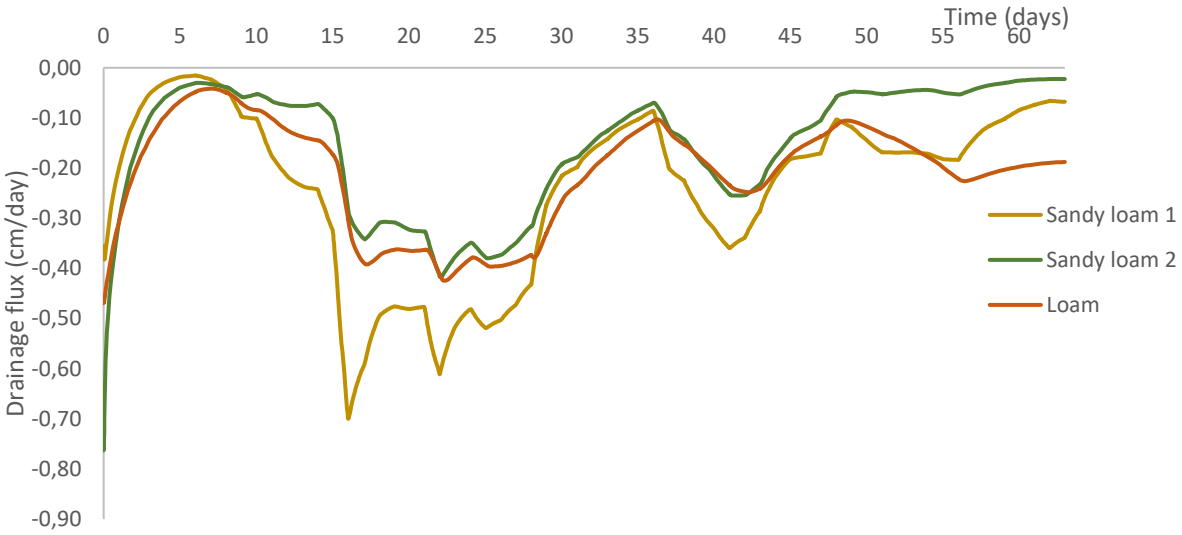

Figure 252: Drainage in sandy loam 1, sandy loam 2 and loam

The figure 32 shows that drainage is higher in the sandy loam 1 soil and lower in the other two types of soil, which reflects the hydraulic properties of the three soils. Drainage in the three types of soil is minimal in the final phase of the second cycle, since the irrigation amounts decreases, as shown in figure 13.

Since root water uptake decreases after applying a 9 dSm^{-1} irrigation, and drainage is also low, it results that the water output in the system is almost zero at the end of the second growth cycle of spinach. Despite the water output being almost zero and there being irrigation, it is not possible to model water contents as high as those observed. This result indicates that the water content observed at this stage is overestimated even after correction.

5. Conclusions

This work intends to model soil salinity in three soils (sandy loam 1, sandy loam 2 and loam) in drip irrigated pot experiments implemented in Lincoln, UK. Using measured soil data that was later corrected, calculated soil evaporation and crop transpiration in standard conditions using *SIMDualKc* and subsequently using *HYDRUS-1D* and applied water and saline stress, resulted in *HYDRUS-1D* modelling for soil water content, EC_{sw}, root water uptake and drainage. The main conclusions are:

- The use of *Canopeo* resulted in good estimates of f_c, evidencing it as a useful tool for estimating f_c from simple pictures from the top of the crops' canopy.
- *SIMDualKc* allowed to obtain soil evaporation and crop transpiration estimates in standard conditions, needed for *HYDRUS-1D* modelling, with the necessary level of accuracy.
- During the course of the experiment, it was noted that high salinity influenced the TDR accuracy. It was attempted to correct the values measured with the TDR by developing correlation functions with soil water content determined by the reference gravimetric method. It was possible to achieve good correlation and to obtained corrected observed values for soil water content.
- Modelling of soil water content and EC_{sw} was successful in all soil types, resulting in relatively low *RMSE*.
- At the end of the second growing cycle, after the 9 dSm^{-1} irrigation, the models underestimated the volumetric soil water content for all soil types. This was likely due to error in the observed data, which, even after correction, was still overestimated in the higher salinity range.
- At the end of the second growing cycle, after the 9 dSm^{-1} irrigation, the models overestimated EC_{sw}. This was due to the corresponding underestimation of the soil water content, resulting in a higher modelled concentration of salts.
- At the end of second cycle, root water uptake and drainage show that water output is nearly zero. Despite the low water outflows and the irrigation, the soil water content modelled is underestimated. This indicates that observed soil water content is still overestimated at high salinity levels even after the correction.

Next steps and recommendations:

- Soil water content measurements should be monitored using a method that is not influenced by salinity in order to obtain accurate values for model calibration.

- To improve the models' accuracy, some points on the water retention curve for each type of soil can be determined, in order to obtain real approximations of the soil's hydraulic parameters.
- Wind speed data should be collected inside the greenhouse, in order to minimize errors in estimating ET_o.
- More information regarding the crop should be collected, such as the plants height and depth of the roots, as well as more photographic records, in order to obtain more accuracy in models.
- Validate the models' using data from new experiments, allowing simulations of short and long-term scenarios.

This work allowed to critically analyse the data resulting from the experimental setup at Lincoln University as well as proposing improvements for monitoring the following phases of the project. It also enabled the development of models with low prediction errors. The developed models will make it possible to simulate the effects of irrigation water quality and future climate conditions on soil salinity in the short and long term, estimating possible productivity losses.

6. Bibliography

Allen, R., Pereira, L., Raes, D., & Smith, M. (1998). Crop evapotranspiration- Guidelines for computing crop water requeirements - FAO Irrigation and drainage paper 56. FAO. Rome, Italy.

Almeida, D. (2006). *Manual das culturas hortícolas* (3rd ed., Vol. 1). Editorial Presença.

Antunes, J., Paz, A. M., Castanheira, N., Gonçalves, M. C., & Cortez, N. (2023). Study of the influence of the standing time in the electrical conductivity of the saturated soil paste. *Revista Ciências Agrárias*. *[accepted for publication]*

Bittelli, M., Salvatorelli, F., & Pisa, P. R. (2008). Correction of TDR-based soil water content measurements in conductive soils. *Geoderma*, *143*(1–2), 133–142. https://doi.org/10.1016/j.geoderma.2007.10.022

Daliakopoulos, I. N., Tsanis, I. K., Koutroulis, A., Kourgialas, N. N., Varouchakis, A. E., Karatzas, G. P., & Ritsema, C. J. (2016). The threat of soil salinity: A European scale review. *Science of The Total Environment*, *573*, 727–739. https://doi.org/10.1016/J.SCITOTENV.2016.08.177

EEA. (2021). *Water resources acroos Europe - confronting water stress: an updated assessment*.

Er-Raki, S., Ezzahar, J., Merlin, O., Amazirh, A., Hssaine, B. A., Kharrou, M. H., Khabba, S., & Chehbouni, A. (2021). Performance of the HYDRUS-1D model for water balance components assessment of irrigated winter wheat under different water managements in semi-arid region of Morocco. *Agricultural Water Management*, *244*(106546). https://doi.org/10.1016/J.AGWAT.2020.106546

FAO. (2021a). *Global map of salt-affected soils*. Rome, Italy, FAO. Available from: https://www.fao.org/documents/card/en/c/cb7247en

FAO. (2021b). *Standard operating procedure for saturated soil paste extract*. Rome, Italy, FAO Available from: https://www.fao.org/publications/card/en/c/CB3355EN/

Feddes, R. A. (1982). Simulation of field water use and crop yield. In F. Penning de Vries & H. van Laar (Eds.), *Simulation of plant growth and crop production* (pp. 194–209).

Fernández, M. D., Bonachela, S., Orgaz, F., Thompson, R., López, J. C., Granados, M. R., Gallardo, M., & Fereres, E. (2010). Measurement and estimation of plastic greenhouse reference evapotranspiration in a Mediterranean climate. *Irrigation Science*, *28*(6), 497–509. https://doi.org/10.1007/s00271-010-0210-z

Fernández, M. D., Bonachela, S., Orgaz, F., Thompson, R. B., López, J. C., Granados, M. R., Gallardo, M., & Fereres, E. (2011). Erratum to: Measurement and estimation of plastic greenhouse reference evapotranspiration in a Mediterranean climate (Irrig Sci, (2010), 28, (497-509), 10.1007/s00271-010-0210-z). *Irrigation Science*, *29*(1), 91–92. https://doi.org/10.1007/S00271-010-0233-5/TABLES/1

Gomes, M. P., & Silva, A. A. (1962). Um novo diagrama triangular para a classificação básica da textura do solo. *Garcia Da Orta*, *10*, 171–179.

Gonçalves, M. C., Martins, J. C., & Ramos, T. B. (2015). A salinização do solo em Portugal. Causas, extensão e soluções. *Revista de Ciências Agrárias*, *38*(4), 574–586. https://doi.org/10.19084/rca15140

Gonçalves, M. C., Ramos, T. B., Šimunek, J., Neves, M. J., Martins, J. C., Pires, F. P., & Leitão, P. (2018). Modelação da dinâmica da água e dos sais num Aluviossolo regado com águas de diferente qualidade: ensaio de validação do modelo HYDRUS-1D com observações em monólitos. *Revista de Ciências Agrárias*, *30*(2), 38–52. https://doi.org/10.19084/rca.15462

González-Esquiva, J. M., Oates, M. J., García-Mateos, G., Moros-Valle, B., Molina-Martínez, J. M., & Ruiz-Canales, A. (2017). Development of a visual monitoring system for water balance estimation of horticultural crops using low cost cameras. *Computers and Electronics in Agriculture*, *141*, 15–26. https://doi.org/10.1016/J.COMPAG.2017.07.001

Gould, I. J., De Waegemaeker, J., Tzemi, D., Wright, I., Pearson, S., Ruto, E., Karrasch, L., Christensen, L. S., Aronsson, H., Eich-Greatorex, S., Bosworth, G., & Vellinga, P. (2021). Salinization threats to agriculture across the North Sea Region. In *Future of Sustainable Agriculture in Saline Environments* (pp. 71–92). CRC Press. https://doi.org/10.1201/9781003112327-5

Gould, I. J., Wright, I., Collison, M., Ruto, E., Bosworth, G., & Pearson, S. (2020). The impact of coastal flooding on agriculture: A case-study of Lincolnshire, United Kingdom. *Land Degradation & Development*, *31*(12), 1545–1559. https://doi.org/10.1002/LDR.3551

Hargreaves, G. H., & Samani, Z. A. (1985). Reference crop evapotranspiration from temperature. *Applied Engineering in Agriculture*, *1*(2), 97–99.

IPCC. (2014). *Climate Change 2014: Synthesis Report Contribution of Working Groups I, II and III to the Fifth Assessment Report of the Intergovernmental Panel on Climate Change*.

Joint Research Centre, Institute for Environment and Sustainability, Tesfai, M., Øygarden, L., Hessel, R. (2015). *Soil threats in Europe*. (M. Tesfai, L. Øygarden, R. Hessel, P. Panagos, S. Kværnø, F. Verheijen, C. Ballabio, J. Stolte, & J. Keizer, Eds.). Publications Office. https://data.europa.eu/doi/10.2788/828742

Kanzari, S., Ben Nouna, B., Ben Mariem, S., & Rezig, M. (2018). Hydrus-1D model calibration and validation in various field conditions for simulating water flow and salts transport in a semi-arid region of Tunisia. *Sustainable Environment Research*, *28*(6), 350–356. https://doi.org/10.1016/J.SERJ.2018.10.001

Kargas, G., & Kerkides, P. (2012). Comparison of two models in predicting pore water electrical conductivity in different porous media. *Geoderma*, *189–190*, 563–573. https://doi.org/10.1016/j.geoderma.2012.06.024

Liu, M., Paredes, P., Shi, H., Ramos, T. B., Dou, X., Dai, L., & Pereira, L. S. (2022). Impacts of a shallow saline water table on maize evapotranspiration and groundwater contribution using static water table lysimeters and the dual Kc water balance model SIMDualKc. *Agricultural Water Management*, *273*(107887). https://doi.org/10.1016/J.AGWAT.2022.107887

Liu, W., Wallis, J., Chichalky, K., Peterson, S., & Richmond, B. (2003). *STELLA* (8). HPS.

Maas, E. (1984). Crop tolerance. *California Agriculture*, *38*(10), 20–21. //calag.ucanr.edu/archive/?article=ca.v038n10p20

Machado, R. M. A., & Serralheiro, R. P. (2017). Soil salinity: Effect on vegetable crop growth. Management practices to prevent and mitigate soil salinization. *Horticulturae*, *3*(30). https://doi.org/10.3390/horticulturae3020030

Mallants, D., Van Genuchten, M. Th., Šimůnek, J., Jacques, D., & Seetharam, S. (2011). Leaching of contaminants to groundwater. *Dealing with Contaminated Sites*, 787–850. https://doi.org/10.1007/978-90-481-9757-6_18

Minhas, P. S., Ramos, T. B., Ben-Gal, A., & Pereira, L. S. (2020). Coping with salinity in irrigated agriculture: Crop evapotranspiration and water management issues. *Agricultural Water Management*, *227*, 105832. https://doi.org/10.1016/J.AGWAT.2019.105832

Patrignani, A., & Ochsner, T. E. (2015). Canopeo: A powerful new tool for measuring fractional green canopy cover. *Agronomy Journal*, *107*(6), 2312–2320. https://doi.org/10.2134/AGRONJ15.0150

Paz, A. M., Amezketa, E., Canfora, L., Castanheira, N., Falsone, G., Gonçalves, M. C., Gould, I., Hristov, B., Mastrorilli, M., Ramos, T., Thompson, R., & Costantini, E. A. C. (2023). Salt-affected soils: field-scale strategies for prevention, mitigation, and adaptation to salt accumulation. *Italian Journal of Agronomy*, *18*(2). https://doi.org/10.4081/ija.2023.2166

Peng, W., Lu, Y., Wang, M., Ren, T., & Horton, R. (2022). Determining water content and bulk density: The heat-pulse method outperforms the thermo-TDR method in high-salinity soils. *Geoderma*, *407*, 115564. https://doi.org/10.1016/j.geoderma.2021.115564

Qiu, R., Du, T., Kang, S., Chen, R., & Wu, L. (2015). Assessing the SIMDualKc model for estimating evapotranspiration of hot pepper grown in a solar greenhouse in Northwest China. *Agricultural Systems*, *138*, 1–9. https://doi.org/10.1016/J.AGSY.2015.05.001

Ramos, T. B., Šimůnek, J., Gonçalves, M. C., Martins, J. C., Prazeres, A., Castanheira, N. L., & Pereira, L. S. (2011). Field evaluation of a multicomponent solute transport model in soils irrigated with saline waters. *Journal of Hydrology*, *407*(1–4), 129–144. https://doi.org/10.1016/j.jhydrol.2011.07.016

Ramos, T. B., Gonçalves, M. C., Martins, J. C., & Pereira, L. S. (2014). Comparação de diferentes funções de pedotransferência para estimar as propriedades hidráulicas dos solos em Portugal. *Actas Do Encontro Anual Da SPCS 2013*, 29–34.

Ramos, T. B., Darouich, H., Šimůnek, J., Gonçalves, M. C., & Martins, J. C. (2019). Soil salinization in very high-density olive orchards grown in southern Portugal: Current risks and possible trends. *Agricultural Water Management*, *217*, 265–281. https://doi.org/10.1016/J.AGWAT.2019.02.047

Ramos, T. B., Darouich, H., Oliveira, A. R., Farzamian, M., Monteiro, T., Castanheira, N., Paz, A., Alexandre, C., Gonçalves, M. C., & Pereira, L. S. (2023). Water use, soil water balance and soil salinization risks of Mediterranean tree orchards in southern Portugal under current climate variability: Issues for salinity control and irrigation management. *Agricultural Water Management*, *283*, 108319. https://doi.org/10.1016/j.agwat.2023.108319

Ramos, T. B., Liu, M., Paredes, P., Shi, H., Feng, Z., Lei, H., & Pereira, L. S. (2023). Salts dynamics in maize irrigation in the Hetao plateau using static water table lysimeters and HYDRUS-1D with focus on the autumn leaching irrigation. *Agricultural Water Management*, *283*(108306). https://doi.org/10.1016/J.AGWAT.2023.108306

Rhoades, J. D., Raats, P. A. C., & Prather, R. J. (1976). Effects of liquid-phase electrical conductivity, water content, and surface conductivity on bulk soil electrical conductivity. *Soil Science Society of America Journal*, *40*(5), 651–655. https://doi.org/10.2136/sssaj1976.03615995004000050017x

Richards, L. A. (1931). Capillary conduction of liquids through porous mediums. *Journal of Applied Physics*, *1*(5), 318–333. https://doi.org/10.1063/1.1745010

Richards, L. A. (1954). *Diagnosis and Improvement of Saline and Alkali Soils* (U.S.Department, Ed.; Agriculture Handbook, Vol. 40). U.S. Gov. Printing Office.

Rosa, R. D., Paredes, P., Rodrigues, G. C., Alves, I., Fernando, R. M., Pereira, L. S., & Allen, R. G. (2012). Implementing the dual crop coefficient approach in interactive software. 1. Background and computational strategy. *Agricultural Water Management*, *103*, 8–24. https://doi.org/10.1016/J.AGWAT.2011.10.013

Rosa, R. D., Ramos, T. B., & Pereira, L. S. (2016). The dual Kc approach to assess maize and sweet sorghum transpiration and soil evaporation under saline conditions: Application of the SIMDualKc model. *Agricultural Water Management*, *177*, 77–94. https://doi.org/10.1016/J.AGWAT.2016.06.028

Saghafi, D., Delangiz, N., Lajayer, B. A., & Ghorbanpour, M. (2019). An overview on improvement of crop productivity in saline soils by halotolerant and halophilic PGPRs. *3 Biotech*, *9*(7), 261. https://doi.org/10.1007/s13205-019-1799-0

Sao, D., Saito, H., Kato, T., & Šimůnek, J. (2021). Numerical analysis of soil water dynamics during spinach cultivation in a soil column with an artificial capillary barrier under different irrigation managements. *Water 2021, Vol. 13, Page 2176*, *13*(16), 2176. https://doi.org/10.3390/W13162176

Šimůnek, J., Van Genuchten, M. T., & Šejna, M. (2012). HYDRUS: model use, calibration, and validation. *Transactions of the ASABE*, *55*(4), 1261–1274. www.hydrus2d.com

Teitel, M., Ziskind, G., Liran, O., Dubovsky, V., & Letan, R. (2008). Effect of wind direction on greenhouse ventilation rate, airflow patterns and temperature distributions. *Biosystems Engineering*, *101*(3), 351–369. https://doi.org/10.1016/J.BIOSYSTEMSENG.2008.09.004

van Genuchten, M. T. (1980). A closed-form equation for predicting the hydraulic conductivity of unsaturated soils 1. *Soil Science Society of America Journal*, *44*, 892–898.

Weil, R. R., & Brady, N. C. (2017). *Nature and properties of soils* (15 th). Pearson Education Limited.

Zeng, W. Z., Xu, C., Wu, J. W., & Huang, J. S. (2014). Soil salt leaching under different irrigation regimes: HYDRUS-1D modelling and analysis. *Journal of Arid Land*, *6*(1), 44–58. https://doi.org/10.1007/S40333-013-0176-9/METRICS

Attachments

Table 122: Kcb and Ke coefficients for each day and for three soil types

Day	K_{cb}	K_e Sandy loam 1	K_e Sandy loam 2	K_e Loam	Growth cycle
1	0.15	1.05	1.05	1.05	1
2	0.15	1.05	1.05	1.05	1
3	0.15	1.03	1.03	1.05	1
4	0.15	1.01	1.01	1.02	1
5	0.15	1.00	1.00	1.02	1
6	0.15	0.99	0.99	1.02	1
7	0.15	0.98	0.98	1.01	1
8	0.15	0.98	0.98	1.00	1
9	0.16	1.04	1.04	1.06	1
10	0.17	0.95	0.95	1.10	1
11	0.16	0.75	0.75	0.93	1
12	0.16	0.59	0.59	0.76	1
13	0.17	0.39	0.39	0.47	1
14	0.30	0.87	0.87	0.78	1
15	0.38	0.91	0.91	0.87	1
16	0.43	0.77	0.77	0.75	1
17	0.52	0.76	0.76	0.74	1
18	0.58	0.67	0.67	0.67	1
19	0.61	0.56	0.56	0.56	1
20	0.67	0.50	0.50	0.50	1
21	0.67	0.38	0.38	0.37	1
22	0.68	0.28	0.28	0.28	1
23	0.93	0.28	0.28	0.28	1
24	0.97	0.33	0.33	0.33	1
25	0.83	0.28	0.28	0.28	1
26	0.87	0.28	0.28	0.28	1
27	0.98	0.31	0.31	0.31	1
28	0.97	0.32	0.32	0.32	1
29	0.98	0.34	0.34	0.34	1
30	0.97	0.31	0.31	0.31	1
31	0.72	0.20	0.20	0.20	1
32	0.91	0.29	0.29	0.26	1
33	0.90	0.33	0.33	0.22	1
34	0.79	0.26	0.26	0.15	1
35	0.15	1.06	1.06	1.06	2
36	0.15	1.10	1.11	1.11	2
37	0.15	0.99	1.00	1.01	2
38	0.15	1.11	1.12	1.13	2
39	0.15	1.01	1.03	1.04	2
40	0.15	1.04	1.06	1.07	2
41	0.15	1.02	1.03	1.04	2
42	0.15	1.05	1.07	1.08	2

Day	K_{cb}	K_e Sandy loam 1	K_e Sandy loam 2	K_e Loam	Growth cycle
44	0.15	1.04	1.04	1.05	2
45	0.15	1.06	1.07	1.07	2
46	0.21	0.98	0.97	0.97	2
47	0.28	0.93	0.93	0.92	2
48	0.31	0.78	0.77	0.77	2
49	0.32	0.60	0.60	0.59	2
50	0.46	0.71	0.71	0.71	2
51	0.57	0.73	0.72	0.72	2
52	0.51	0.53	0.53	0.52	2
53	0.68	0.56	0.56	0.56	2
54	0.70	0.47	0.47	0.46	2
55	0.78	0.42	0.42	0.41	2
56	0.73	0.29	0.29	0.29	2
57	0.85	0.24	0.24	0.24	2
58	0.90	0.30	0.30	0.30	2
59	0.99	0.34	0.34	0.33	2
60	0.87	0.29	0.29	0.29	2
61	0.94	0.32	0.29	0.29	2
62	0.96	0.35	0.32	0.32	2
63	1.00	0.40	0.36	0.35	2
64	0.96	0.44	0.34	0.34	2
65	0.82	0.40	0.29	0.28	2
66	0.88	0.48	0.36	0.34	2
67	0.84	0.47	0.32	0.35	2
68	0.86	0.44	0.26	0.34	2
69	0.79	0.30	0.23	0.28	2